



Early Paleozoic juvenile crustal growth in the Paleo-Asian Ocean: A contribution from the Zasur'ya accretionary complex of NW Altai

Inna Safonova^{a,b,*}, Anastasiya Krutikova^{a,c,*}, Alina Perfilova^{a,c}, Olga Obut^d, Victor Kovach^e, Anna Kulikova^c

^a Novosibirsk State University, 1 Pirogova St, Novosibirsk 630090, Russia

^b Southwest Jiaotong University, Xi'an Road 999, Chengdu 611756, China

^c Sobolev Institute of Geology and Mineralogy SB RAS, Koptyuga ave. 3, Novosibirsk 630090, Russia

^d Trofimuk Institute of Petroleum Geology and Geophysics SB RAS, Koptyuga ave. 3, Novosibirsk 630090, Russia

^e Institute of Precambrian Geology and Geochronology, Russian Academy of Science, Makarova Emb, 2, St. Petersburg 199034, Russia

ARTICLE INFO

Keywords:

Central Asian Orogenic Belt
Altai orogen
Charysh-Terekta suture-shear zone
Geochemistry
U–Pb zircon ages
Hf-in-zircon isotopes
Bulk-rock Nd isotopes

ABSTRACT

Reconstruction of proportions between juvenile and recycled crust remains challengeable because a big part of juvenile source magmatic rocks formed at intra-oceanic arcs, can be destroyed by surface and tectonic erosion leaving, at best, greywacke sandstones. Such sandstones are typically hosted by accretionary complexes, which study, therefore, is of crucial importance. In this paper we review available geological and micropaleontological data and present first U–Pb detrital zircon ages, geochemical data and isotope (Sm–Nd, Lu–Hf) data from sandstones of the late Cambrian–early Ordovician Zasur'ya accretionary complex (AC) of NW Altai. No island-arc units have ever been reported there. The Zasur'ya AC includes ocean plate stratigraphy (OPS) magmatic and sedimentary rocks of three formations, Listvenny (l. Cambrian), Talitsa (Tremadocian) and Marcheta (Floian), which age was constrained by microfossils. The OPS assemblage includes basalt, pelagic chert and hemipelagic siliceous mudstone and siltstone, and sandstone. We analyzed zircons in five samples. The distributions of U–Pb ages of detrital zircons from five samples of sandstones are all unimodal with main peaks at ca. 488 Ma (Listvenny Fm.), 491 Ma (Talitsa Fm.) and 485 Ma (Marcheta Fm.). The Precambrian ages are very few. The maximum deposition ages inferred from the youngest populations of zircon ages are ca. 464 Ma. Compositionally, the sandstones are greywackes or feldspar litharenites. The Listvenny and Talitsa sandstones are higher silicic ($\text{SiO}_{2\text{av.}} = 68.5 \text{ wt\%}$) compared to Marcheta samples ($\text{SiO}_{2\text{av.}} = 60.5 \text{ wt\%}$). The major and trace element features of all sandstones are similar to supra-subduction intermediate-felsic (Listvenny, Talitsa) and mafic-intermediate (Marcheta) magmatic rocks. All samples yielded positive values of zircon $\epsilon\text{HF}(t)$ (+4.3 to +20.1) and bulk-rock $\epsilon\text{Nd}(t)$ (+0.6 to +4.8) indicating juvenile magmatic rocks in the provenance. However, the Listvenny and Talitsa samples show lower $\epsilon\text{Nd}(t)$ (1.3 and 0.8, respectively) than those of the Marcheta Fm. (4.7). Probably the Zasur'ya sandstones were deposited in a back-arc basin (Listvenny, Talitsa), and fore-arc basin (Marcheta). All Zasur'ya greywacke sandstones were derived by destruction of a single late Cambrian–Early Ordovician intra-oceanic arc. The Zasur'ya intra-oceanic arc was identified in NW Altai for the first time and it represents a new site of juvenile crustal growth in the CAOB.

1. Introduction

Greywacke sandstones of supra-subduction and accretionary complexes represent an invaluable source of information about their parental magmatic protoliths, that were emplaced either at intra-oceanic, or at continental arcs that once existed at Pacific-type active convergent margins of paleo-oceans. Intra-oceanic arcs produce major

volume of juvenile crust compared to continental arcs (Defant and Drummond, 1990; Kelemen et al., 1995; Stern, 2010; Gazel et al., 2015). Identification of those arcs is of key importance for reconstructing the proportions of juvenile and recycled crust in intra-continental orogenic belts that formed as a result of the evolution and closure of paleo-oceans. However, direct study of those arcs may appear challengeable due to their surface or tectonic erosion (e.g., Cliff and Vannucchi, 2004; Scholl

* Corresponding authors at: Novosibirsk State University, 1 Pirogova St, Novosibirsk 630090, Russia.

E-mail addresses: inna03-64@mail.ru (I. Safonova), a.krutikova20@gmail.com (A. Krutikova).

<https://doi.org/10.1016/j.earscirev.2023.104648>

Received 29 June 2023; Received in revised form 25 October 2023; Accepted 2 December 2023

Available online 14 December 2023

0012-8252/© 2023 Elsevier B.V. All rights reserved.

and von Huene, 2007; Stern and Scholl, 2010). A solution may come from study of greywacke sandstones formed by direct destruction of magmatic arcs. Recently, more and more geochronological, geochemical and isotope data have been obtained from such sandstones hosted by modern and old supra-subduction and accretionary complexes (e.g., Jiang et al., 2011; Long et al., 2012; Konopelko et al., 2021a; Hu et al., 2022; Perfilova et al., 2022; Safonova et al., 2021, 2022). These data gave us a clue to the reconstruction of new juvenile intra-oceanic arcs. U—Pb ages of detrital zircons from sandstones provide constraints on the age of magmatic rocks in the source areas. In addition, U—Pb detrital zircon data help to define maximal depositional ages, which can contribute to better understanding of regional stratigraphy, because such sandstones seldom carry well-preserved microfossils. Petrographic, geochemical and isotopic characteristics of greywacke sandstones would allow us to infer the composition and petrogenesis of parental magmatic rocks and, finally, to reconstruct the type of parental arc, intra-oceanic

or continental. Such reconstructions are important to develop reliable tectonic models and further related models for orogeny-related ore mineralization.

In fossil Pacific-type orogenic belts greywacke sandstones typically occur as parts of accretionary and supra-subduction complexes. The Central Asian Orogenic Belt (CAOB), the world largest accretionary orogen, that formed by the suturing of the Paleo-Asian Ocean (e.g., Zonenshain et al., 1990; Sengör et al., 1993; Dobretsov et al., 2003; Safonova, 2009) consists of numerous island-arc and continental arc terranes including supra-subduction and accretionary complexes, microcontinents, fore-arc and back-arc turbidite basins, intra-plate volcanic and plutonic belts (Berzin et al., 1994; Didenko et al., 1994; Buslov et al., 2001, 2002; Windley et al., 2007; Xiao et al., 2004, 2010; Safonova et al., 2017). Although the CAOB has been studied by many research teams worldwide, the proportions of juvenile and recycled crust in the Central Asian Orogenic belt, remain debatable (Kröner et al.,

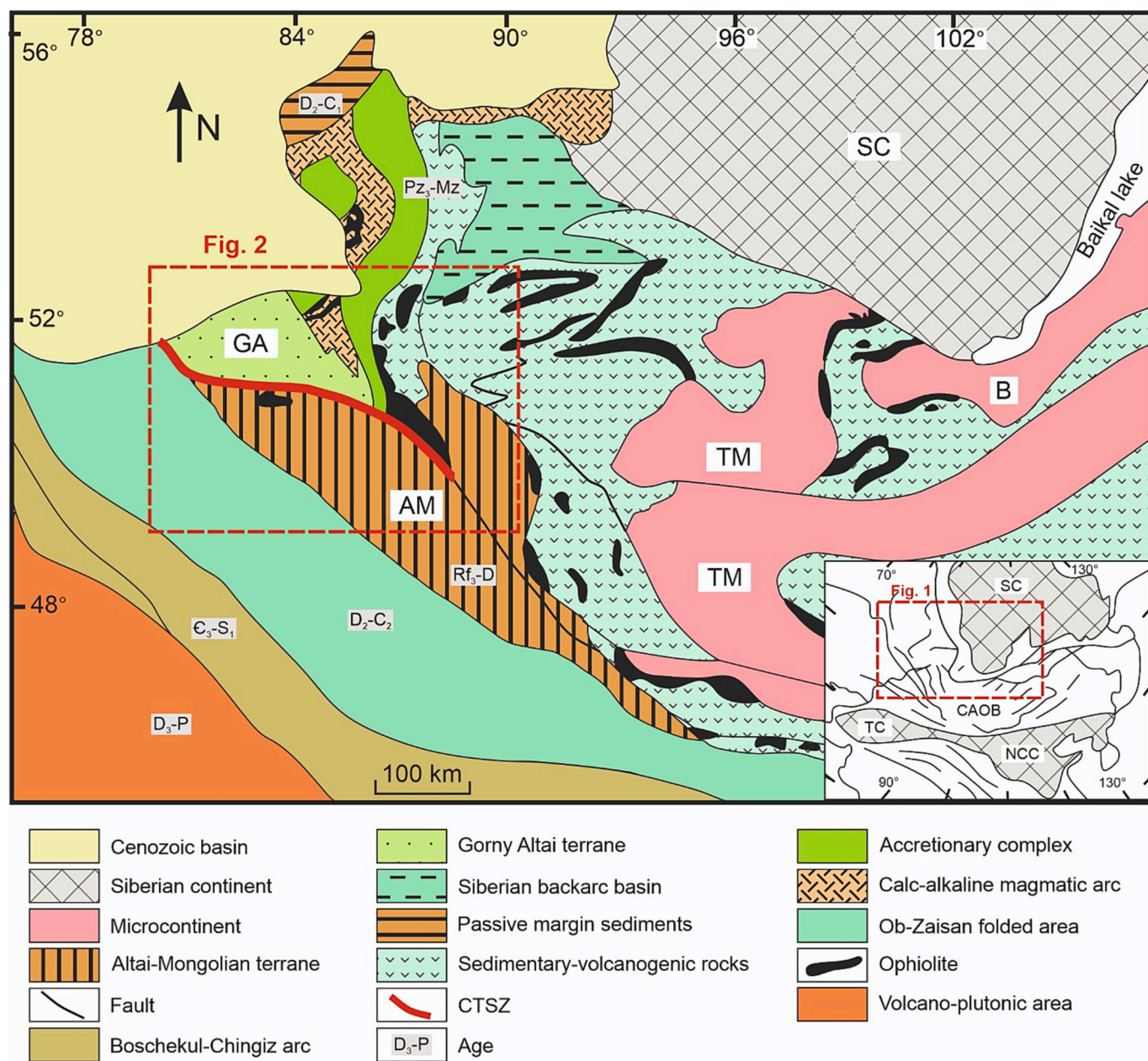


Fig. 1. Simplified geological scheme of the western Central Asian Orogenic Belt (CAOB, adapted from Buslov and Safonova, 2010). Insert: tectonic outline of the CAOB. Abbreviations: AM, Altai-Mongolian; B, Barguzin; CTSZ, Charysh-Terekta suture-shear zone; GA, Gorny Altai; NCC, North China continent; SC, Siberian continent; TC, Tarim continent; TM, Tuva-Mongolian.

2014, 2017; Safonova, 2017). The precise evaluation of such proportions is necessary for developing new and upgrading former regional to global models of geodynamic evolution and mineral exploration. Recently, several new intra-oceanic arcs have been identified in the western CAOB (Safonova et al., 2017, 2018, 2020; Degtyarev et al., 2021a), including those reconstructed from greywacke sandstones (Safonova et al., 2021, 2022; Safonova and Perfilova, 2023). However, other results still show a big portion of recycled crust in the CAOB., Evidence for that comes from U—Pb detrital zircon ages, which spectra/histograms show both Paleozoic peaks with positive to negative $\epsilon_{\text{Hf}}(t)$ in zircon and Precambrian zircons, plus isotopic studies of igneous rocks, whole-rock Nd and Hf-in-zircon, showing either only negative or both negative to positive values of $\epsilon_{\text{Nd}}(t)$ and $\epsilon_{\text{Hf}}(t)$ (e.g., Degtyarev et al., 2017; Biske et al., 2019; Ganbat et al., 2021; Konopelko et al., 2021a, 2021b; Alexeiev et al., 2023; Wang et al., 2023). Such isotope data indicate participation of recycled crust material in magma generation.

In this paper we present first geochronological, geochemical and Hf and Nd isotope data from sandstones of the Zasur'ya accretionary complex or terrane of the Charysh-Terekta suture-shear zone in the northwestern Altai, a region in the western CAOB (Fig. 1). In addition, we review available geological and biostratigraphical (radiolarians and conodonts) data from that geological structure (Supplementary Tables S1, S2) (Iwata et al., 1997; Sennikov et al., 2003, 2011; Krutikova et al., in press). The new age data partly disagree with the available micro-paleontological data thus requiring revision of the stratigraphic subdivision of the Zasur'ya AC. Our new geochemical and isotope data reveal that the Zasur'ya sandstones formed by destruction of late Cambrian to Early Ordovician mafic to felsic magmatic rocks of supra-subduction origin with juvenile source characteristics. We document at least one, possibly two intra-oceanic arcs, which fully disappeared from the surface as magmatic bodies. Such an intra-oceanic arc has never been recognized in the study area before and definitely shifts the juvenile-recycled crust balance in the CAOB to the juvenile side.

2. Tectonic framework of northwestern Altai

North-western Altai is a part of the Altai orogenic belt or orogen extended over the territories of four countries: China, Kazakhstan, Mongolia and Russia (e.g., Cunningham et al., 1996; Li and Poliyangsi, 2001; Buslov et al., 2001; Windley et al., 2002; Safonova, 2014). The Altai orogen is located in the western CAOB and is linked to the late Neoproterozoic-early Paleozoic evolution of the Paleo-Asian Ocean, PAO (Dobretsov et al., 2003; Buslov et al., 2001; Safonova, 2014). In general, the early Paleozoic structures of the western CAOB are dominated by island arc terranes once formed at active margins of the PAO (Seley-Urumbai, Boshchekul-Chingiz, Tekturmas, Itmurundy, Songkul), and microcontinents, Kokchetav, Aktau-Mointy, North Tienshan, Junggar and Altai-Mongolian (e.g., Buslov et al., 2001; Li and Poliyangsi, 2001; Windley et al., 2007; Degtyarev, 2011; Jiang et al., 2011; Safonova, 2014, 2017; Liu et al., 2016; Alexeiev et al., 2020, 2023; Konopelko et al., 2021a, 2021b). In the territory of Russia, the Altai orogen is considered as the western part of the Altai-Sayan folded area (ASFA), which, in general, represents an accretionary-collisional belt formed at the junction zone of the Siberian and Kazakhstan continents, which approached each other during the middle-late Paleozoic evolution and closure of the PAO (e.g., Zonenshain et al., 1990; Berzin et al., 1994; Dobretsov et al., 2003; Safonova et al., 2017).

The ASFA has a complicated, mosaic-type structure consisting of microcontinents built upon Precambrian basements, Neoproterozoic-early Paleozoic island-arc and active continental margin terranes, accretionary complexes and their hosted fragments of oceanic crust or, in other words, units of ocean plate stratigraphy (e.g., Li et al., 2007; Buslov et al., 2002; Safonova, 2009; Glorie et al., 2011) (Fig. 1). The structure of the ASFA records two important collisional stages: the late Devonian-early Carboniferous collision of the Altai-Mongolian terrane with the Siberian continent and the late Carboniferous-Permian collision

of the Kazakhstan and Siberian continents (Buslov et al., 2001).

The Altai orogen formed at the south-western active margin of the Siberian continent and represents an early stage of the formation of CAOB continental crust. The tectonic structure of Altai is also a collage of terranes formed in different tectonic settings and at different stages of the evolution of the PAO. The Altai orogen consists of late Neoproterozoic to early Paleozoic supra-subduction complexes including accreted oceanic crust (accretionary complexes), continental arc and intra-oceanic arc, and fore-arc terranes (e.g., Buslov et al., 2001, 2002; Safonova et al., 2008, 2011a, 2011b; Kruk et al., 2018; Safonova, 2014). The terranes are separated from each other by late Paleozoic thrust faults and strike-slip faults (Buslov et al., 2004). The Altai orogen is a key area to understand the establishment of late Neoproterozoic-early Paleozoic juvenile versus continental crust of the CAOB, in particular, the proportions of juvenile and recycled crust (e.g., Kovalenko et al., 2004; Xiao et al., 2004; Windley et al., 2007; Safonova, 2017).

A major tectonic structure of northwestern Altai is a reactivated suture-shear zone named Charysh-Terekta (Buslov et al., 2001) or Charysh-Terekta-Ulagan (Glorie et al., 2011). The 130–150 km long Charysh-Terekta suture-shear zone (CTSZ) is bordered by the Altai-Mongolian and Gorny Altai terranes, both parts of the ASFA, in the east and south, respectively, and by the Rudny Altai terrane, a part of the Ob'-Zaisan folded area, in the west (Figs. 1, 2). The CTSZ is separated from the Gorny Altai terrane by the Baschelak fault and from the Rudny Altai terrane by the North-Eastern fault (Fig. 2). The CTSZ formed by the late Devonian collision of the Altai-Mongolian microcontinent and Siberian continent (Fig. 1) (Buslov et al., 2001).

Five structural-formational units have been recognized in the CTSZ (from west to east): Inya, Kur'ya-Akimov, Charysh, Zasur'ya, and Maralikhka (Fig. 3). The units are separated by zones of intensive shearing and greenschist metamorphism. Each unit is dominated by a specific set of lithologies formed in different tectonic settings. The Inya Unit consists of middle-late Cambrian-polymictic terrigenous sedimentary rocks (sandstones) of the Suetka Formation, possibly derived from an island arc, and fore-arc Ordovician-Silurian carbonate rocks and terrigenous-carbonate rocks (Buslov et al., 2000). The Kur'ya-Akimov Unit is dominated by early-middle Devonian volcano-sedimentary rocks probably formed at an active margin similar to that described in the adjacent Gorny Altai terrane (Buslov et al., 2002; Safonova, 2014). The Charysh Unit consists of Middle-Late Ordovician tuffs, sandstones, siliceous mudstones and siltstone, that form, in places, turbidite-like rhythmically bedded packages. These volcanogenic-sedimentary rocks possibly deposited in a forearc trough.

The Zasur'ya Unit is dominated by late Cambrian-Early Ordovician sedimentary and igneous rocks of oceanic origin (e.g., Iwata et al., 1997; Buslov et al., 2000; Sennikov et al., 2003). The sedimentary rocks are dominantly chert, siliceous mudstone and siltstone, and sandstone. The igneous rocks are basalts possessing geochemical affinities of oceanic island basalts (OIB) and mid-oceanic ridge basalts (MORB) (Buslov et al., 2001; Safonova et al., 2011a). The Zasur'ya Unit has sheared and deformed boundaries with the surrounding Charysh and Maralikhka units (Fig. 3). The Maralikhka Unit (also referred to as Talitsa Unit in Buslov et al., 2000) takes the easternmost position in respect to the other units and occupies the largest area (Fig. 3). It consists of dark-grey phyllites, siliceous mudstones and siltstones and sandstones. The sandstones and siliceous sedimentary rocks also form turbiditic associations. The sandstones consist of poorly rounded clasts of volcanic rocks, chert, siliceous mudstone, quartz and feldspar submerged into sericite-chlorite-siliceous matrix (Buslov et al., 2000). In this paper, we will focus on the Zasur'ya Unit (Isozaki et al., 1990; Safonova et al., 2011a; Safonova and Santosh, 2014), with a special emphasis to the first data obtained from siliciclastic/terrigenous rocks (sandstones) associated with OPS igneous and sedimentary rocks (Supplementary Fig. S1, Table S1).

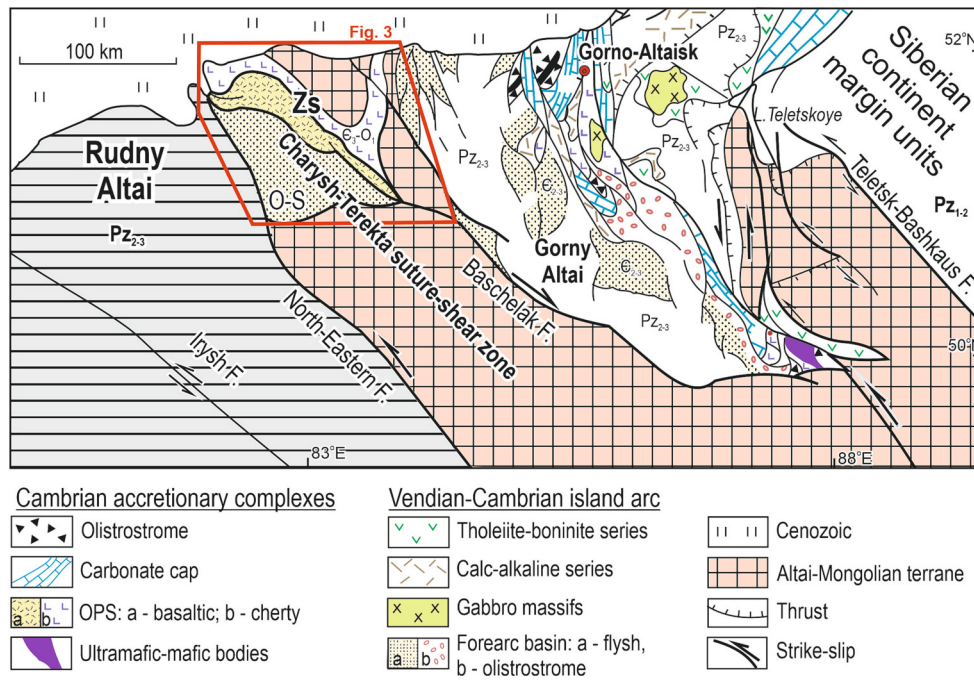


Fig. 2. Tectonic scheme of the Altai-Sayan Folded Area (ASFA) (modified from Buslov et al., 2001). F, fault; OPS, Ocean Plate Stratigraphy; Zs, Zasur'ya AC.

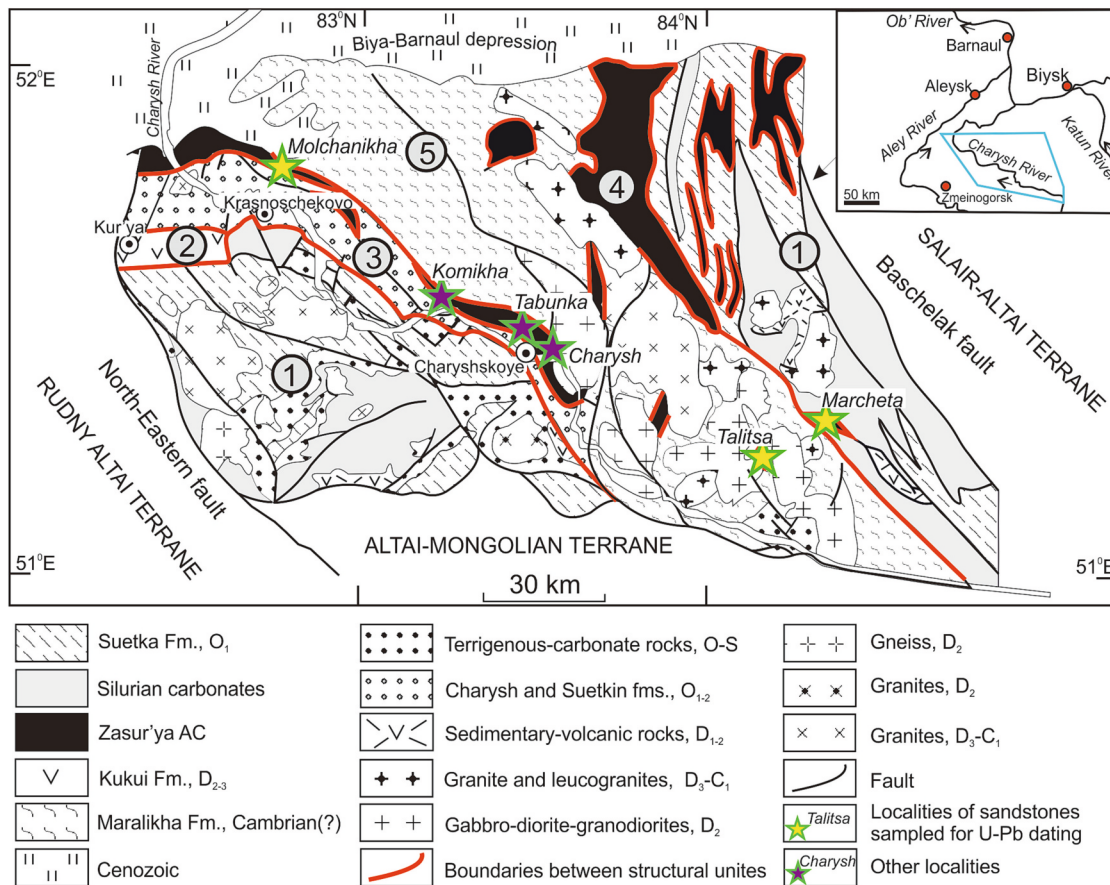


Fig. 3. Geology and structure of the northwestern Charysh-Terehta suture-shear zone; modified from Buslov et al., 2001. Numbers in circles are for structural units: 1, Inya; 2, Kur'ya-Akimov; 3, Charysh; 4, Zasur'ya; 5, Talitsa.

3. Zasur'ya accretionary complex: lithology and stratigraphy

3.1. The nature of the Zasur'ya Series

The nature of the Zasur'ya Unit has been remaining a matter of debates since the late 1990-ties. The first group of scientists (e.g., Buslov et al., 1999, 2000, 2001; Glorie et al., 2011; Buslov, 2011) considered the Zasur'ya Unit as an exotic terrane squeezed between two terranes, Rudny Altai and Gorny Altai, and located at the north-western tip of the extended Charysh-Terekta-Ulagan-Sayan suture. The second group of scientists referred the sedimentary and igneous rocks of this unit to as Zasur'ya Formation or Suite (Iwata et al., 1997) and then, later, Zasur'ya Series (Sennikov et al., 2003). Later, I. Safonova with co-authors (Safonova et al., 2004, 2011a; Safonova and Santosh, 2014) recognized a succession of ocean plate stratigraphy there (OPS; Isozaki et al., 1990): basalt (MORB) – pelagic sediments (radiolarian, ribbon chert), hemipelagic sediments (siliceous shale, mudstone, siltstones), trench sediments (turbidites) and oceanic island facies (OIB, epiclastic slope facies). More evidence for the accretionary nature of the Zasur'ya Unit comes from careful mappings of OPS sediments at key outcrops of NW Altai showing their almost vertical bedding and repeated packages of chert-shale-sandstone resembling the thrust-duplex structures (Krutikova et al., in press). Such structures are typical of all accretionary complexes, both younger complexes of the western Pacific (e.g., Isozaki et al., 1990; Ueda, 2005; Wakita, 2012; Safonova et al., 2016) and older ones of Central Asia and worldwide (e.g., Komiya et al., 1999; Maruyama et al., 2010; Kusky et al., 2013; Burg, 2018; Safonova et al., 2020).

The Zasur'ya OPS succession from basalt to pelagic cherts, siliceous hemipelagites and sandstones and the high-angle to vertical bedding of the sediments confirm the accretionary nature of the Zasur'ya Series. Consequently, as the Zasur'ya Unit hosts accreted OPS rocks and consists of tectonic sheets of deep-sea oceanic sediments and volcanic rocks erupted over the oceanic floor or at oceanic islands, in this paper we refer it to as accretionary complex (AC).

In a wide sense, the Zasur'ya AC hosts fragments of the late Cambrian-Early Ordovician crust of the Paleo-Asian Ocean (Safonova et al., 2011a). The sedimentary formations of the Zasur'ya AC occur in tectonic contacts with surrounding Cambrian (?) and Late Ordovician-Silurian terrigenous and terrigenous-carbonate rocks of the Charysh and Maralikhka units (section 2, Fig. 3). The Cambrian age of the rock formations surrounding the Zasur'ya AC remains questioned, as no microfauna have been found there so far. The previous researchers considered those formations as Cambrian judging by geological and structural relationships (Buslov et al., 2000; Sennikov et al., 2003, 2018). As a result, the age boundaries of the formations and the source of the sandstones remain not well identified.

3.2. Stratigraphy and lithology

The Zasur'ya AC include mostly sedimentary rocks of the Zasur'ya Series, that, according to Sennikov and co-authors (Sennikov et al., 2003, 2011) consists of three formations (bottom to top): Listvenny, Talitsa and Marcheta (Fig. 4). All three formations are dominated by sedimentary rocks with a subordinate amount of volcanic and sub-volcanic rocks (Buslov et al., 1999, 2000; Sennikov et al., 2003; Safonova et al., 2011a). In general, the sedimentary rocks are dominated by pelagic chert, hemipelagic siliceous shale, mudstone and siltstones, and sandstones. The pelagic and hemipelagic sediments carry late Cambrian – Early Ordovician radiolarians and conodonts (supplementary Tables S1, S2) (Iwata et al., 1997; Sennikov et al., 2011).

The lower Listvenny Fm., which rocks are outcropped in the northern and central parts of the Zasur'ya Unit (Fig. 3), consists of basalts, pelagic cherts, hemipelagic siliceous shales and mudstones, and coarser-grained terrigenous rocks, siltstone and sandstone (Fig. 4). The small outcrops of basaltic flows (Fig. 5A) and pillow-lavas are (seldom outcropped) in

contact with red, grey-brown, violet and grey ribbon cherts (Fig. 5B). The cherts are typically overlapped by red-brown and grey mudstones and siltstones intercalated with greenish-grey and grey sandstones (Figs. 4, 5C). The cherts and siliceous shales associated with basalts show signatures of down-slope slumping as semi-sphere textures (10–20 cm), *syn*-sedimentary epiclastic Z-folding (Fig. 5D), and brecciation. Such structures and textures and the geochemical affinities of the underlying basalts suggest their deposition on slopes of an oceanic rise (island, seamount) (Safonova et al., 2011a; Sennikov et al., 2011). The red cherts of the Listvenny Fm. contain late Cambrian radiolarians and conodonts, Aksay and Batyrbai ages according to the Russian Stratigraphic Code (Sennikov et al., 2003, 2018; Stratigraphic Code of Russia, 2006).

The middle Talitsa Fm. crops out in the central and south-eastern part of the Zasur'ya Unit (Fig. 3). It consists of alternated packages of grey, greenish and motley shales, mudstones, siltstones and sandstones (Fig. 4, 5E). The subordinate basalts are also compositionally similar to OIB (Iwata et al., 1997; Buslov et al., 2001; Safonova et al., 2011a). In addition, there are also volcanic rocks associated with sandstones, which composition is close to supra-subduction basalt Supplementary Table S2, but only one sample has been identified and studied so far (sample TLC-21-05). The lower stratigraphic boundary of the formation has not been well-defined and is arbitrary considered as lower Tremadocian. The siliceous mudstones of the upper part of the Talitsa Fm. carry late Tremadocian-Floian radiolarians and conodonts (Sennikov et al., 2015).

The sedimentary rocks of the Marcheta Fm. are exposed in the south-eastern part of the Zasur'ya Unit (Fig. 3). The dominating lithologies are pelagic chert, hemipelagic siliceous sedimentary rocks and sandstones plus tuffs and tuffaceous sandstones (Fig. 4). No igneous rocks in direct contact with paleontologically dated sediments have been found so far. The red and red-brown cherts have massive and ribbon textures (Fig. 5F). The cherts, together with greenish-grey, grey and tobacco-grey siltstones (Fig. 5G) and grey to dark-grey poorly sorted sandstones (Fig. 5H), form repeated packages resembling turbidites (Fig. 5I). The bedding of all packages is almost vertical. The siltstones often look strongly sheared (Fig. 5G). Red cherts contain Tremadocian-Floian conodonts, radiolarians and siliceous sponge spicules (Sennikov et al., 2011, 2015; Obut, 2023).

The sandstones of all three formations, the foci of this paper, occur as packages with deep-sea sediments (chert, siliceous shale, etc.) having high-angle to almost vertical bedding. The contacts between the packages are typically covered by vegetation and represent shallow dry valleys (Krutikova et al., in press). We sampled sandstones of the Listvenny, Talitsa and Marcheta formations at the Molchanikhka, Talitsa and Marcheta localities, respectively (Supplementary Table S1; Fig. 3; Fig. S1).

3.3. Description of sampling localities

The Molchanikhka Locality is situated in the northern part of the Zasur'ya AC and includes outcrops of sedimentary rocks of the Listvenny Fm., red to brown ribbon chert, locally quartzitised, grey to brown-grey siliceous mudstones and dark to light grey sandstones. The cherts and mudstones are present in almost equal amounts, the sandstones are less voluminous. The cherts host microfossils, late Cambrian (Batyrbai according to the Russian Stratigraphic Code) radiolarians and conodonts (Sennikov et al., 2011). The sandstones occur in the upper parts of the repeated packages together with chert and siliceous mudstones (Fig. 4) and visually resemble greywackes as their clasts are poorly sorted and poorly rounded. The SWW-striking sedimentary packages dip at high angles. In places, the siliceous mudstones and sandstones rhythmically alternate. The thickness of sandstone beds varies from 2 to 20 m.

The Talitsa Locality is more to the south-east (Fig. 3). The dark-grey or green sandstones (Fig. 5E) are associated with siliceous mudstones, siltstones and chert of the Talitsa Fm. (Fig. 4) and with volcanic rocks of unclear origin. The cherts are subordinate in volume (less 2%). The

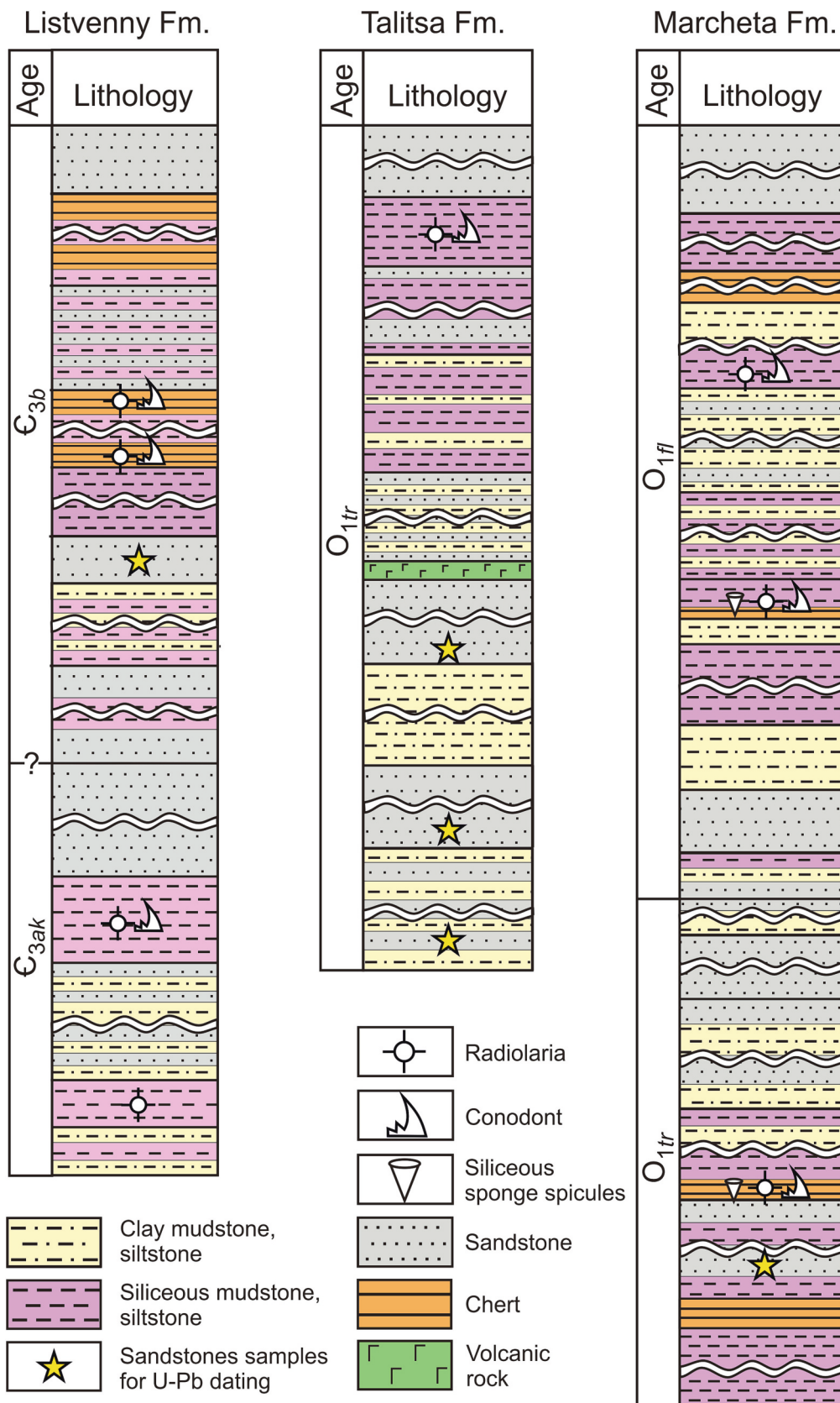


Fig. 4. Generalized lithology-stratigraphic columns of the Listvenny, Talitsa and Marcheta formations (compiled based on the data from Sennikov et al., 2011).



Fig. 5. Field photos: A, small outcrop of OIB-type basalt; B, basalt in contact with chert; C, contact between pelagic chert and hemipelagic mudstone; D, slope sediments with Z-folds; E, sandstones (TLC-21-15); F, ribbon chert; G, contact between sandstone and siliceous mudstone; H, sandstones with block structure (MR-20-02/2); I, turbidites. Formations: A-D, Listvenny Fm.; E, Talitsa Fm.; F–I – Marcheta Fm.

siliceous mudstones and siltstones have tiled and massive textures. In the upper part of the section, the sedimentary rocks show clear signatures of contact metamorphism to form cordierite hornfels as a result of intrusion of late Carboniferous granitoids (Fig. 3) (Vladimirov et al., 2008). The siliceous mudstones of this locality carry Tremadocian conodonts and radiolarians (Sennikov et al., 2011). The boundaries between different lithologies are covered by vegetation.

The Marcheta Locality is also situated in the southeastern part of the Zalur'ya AC, about 30 km northeast of the Talitsa Locality. The SE-striking vertical to subvertical sedimentary strata are dominated by cherts, siliceous claystone, thin-bedded mudstone, siltstone and grey and greenish-grey poorly sorted fine to coarse-grained sandstones of the Marcheta Fm. (Fig. 5). The fine-grained (Fig. 5F-I) and coarse-grained (Fig. 5H) sandstones have bedded and massive textures, respectively. The fine-grained varieties are often intercalated with mudstones or siltstones. The chert and siliceous claystone have ribbon textures. Conodonts and radiolarians from the siliceous mudstones are of Tremadocian and Floian ages (Sennikov et al., 2011). All these lithologies form repeated packages separated by faults. We documented direct contacts between chert and siliceous claystone or mudstone and between sandstones and siltstones (Fig. 5I).

For geochronological, geochemical and isotope studies we sampled sandstones at as large as possible exposures with minimal amounts of cracks filled by quartz and carbonates and showing lower degrees of

secondary alteration. The best samples were selected for petrography and bulk-rock studies: U–Pb zircon dating, X-ray fluorescence for major elements, ICP MS for rare elements and bulk-rock Sm–Nd isotopes and Lu–Hf in zircon. For details on methods and analytical procedures see Suppl. Electr. materials.

4. U–Pb geochronology of detrital zircons

U–Pb ages were determined in zircons from 5 samples of sandstones of the Listvenny Fm., (Molchanikha Locality; sample SSS-4/1), Talitsa Fm. (Talitsa Locality; samples TLC-21-15,16,18) and Marcheta Fm. (Marcheta Locality; sample MR-20-02.2) (Supplementary Table S1; Fig. 6). The isometric to prismatic zircon grains are dominantly transparent, some slightly yellowish. The angular shape of the grains suggests their short-distant transportation and fast burial (Supplementary Fig. S2). In CL photos, most zircons reveal magmatic-type (oscillatory) zoning (Supplementary Fig. S2); the size of grains is between 50 and 180 μm . Th/U values span 0.16 to 1.9, also confirming their magmatic genesis (Hanchar and Hoskin, 2003) (Supplementary Figs. S2, S3). Totally, we analyzed 540 detrital zircons from Zalur'ya sandstones (Supplementary Table S3). In the $^{207}\text{Pb}/^{235}\text{U}$ - $^{206}\text{Pb}/^{238}\text{U}$ concordia diagram, most points also plot very close to the concordia or a bit to the right of it (Fig. 6).

One hundred forty zircons were analyzed in sample SSS-4/1

(Molchanikha Locality, Listvenny Fm.), of which 131 showed concordant $^{207}\text{Pb}/^{235}\text{U}$ and $^{206}\text{Pb}/^{238}\text{U}$ ratios within $\pm 5\%$ (Supplementary Table S3). In the $^{207}\text{Pb}/^{235}\text{U}$ - $^{206}\text{Pb}/^{238}\text{U}$ concordia diagram, the points plot in the interval from 650 to 450 Ma (Fig. 6A). The histogram and probability curve distribution of U–Pb ages is unimodal showing a main peak at 520–460 Ma ($N = 111$), plus a much smaller peak at 650–610 Ma ($N = 7$) and two groups of Precambrian ages clustered at 2360–1855 Ma ($N = 7$) and 875–760 Ma ($N = 6$) (Fig. 6B). The total amount of the Precambrian ages is about 13%. The weighted average of the main peak is 487.4 ± 3.1 Ma (late Cambrian). The youngest grains range in age from 468 to 465 Ma ($N = 6$). The weighted average of the youngest cluster is 465.7 ± 5.1 Ma, i.e., Late Ordovician (Fig. 7A).

In the three samples of sandstones from Talitsa Locality (Talitsa Fm.), we analyzed 293 grains, of which 290 yielded concordant U–Pb ages (Supplementary Table S3). In the $^{207}\text{Pb}/^{235}\text{U}$ - $^{206}\text{Pb}/^{238}\text{U}$ concordia diagram, most points span the interval from 550 to 450 Ma (Fig. 6C). The distribution of the U–Pb ages is also unimodal showing a main cluster at ca. 560–460 Ma ($N = 251$) with a weighted average of 491.2 ± 2.1 Ma (late Cambrian) (Fig. 6D). The oldest zircons are ca. 2881 and 2069 Ma, about 10% of the whole population of U–Pb ages. The age of the youngest zircons spans 465 to 463 Ma ($N = 6$). The weighted average of the youngest cluster is 464.0 ± 6.9 Ma, i.e., also Late Ordovician (Fig. 7B).

In sample MR-20-02/2 (Marcheta) we analyzed 107 grains with 98 ratios concordant at $\pm 5\%$ (Table S2). In the $^{207}\text{Pb}/^{235}\text{U}$ - $^{206}\text{Pb}/^{238}\text{U}$ concordia diagram, most points span the interval from 550 to 450 Ma (Fig. 6E). The distribution of the U–Pb ages is also unimodal showing a main cluster at 520–460 Ma ($N = 93$) (Fig. 6F). The oldest zircons are of ca. 534 and 548 Ma, i.e., almost nil Precambrian ages. The weighted average of the main peak is 485.4 ± 3.9 Ma (exactly the border between the late Cambrian and Early Ordovician). The youngest grains range in age from 466 to 464 Ma ($N = 6$). The weighted average of the youngest cluster is 464.7 ± 5.3 Ma (Fig. 7C).

5. Petrography

We chose 27 sandstones sampled at the Molchanikha, Talitsa and Marcheta localities of the Zalur'ya AC (Fig. 3) for detailed petrographic descriptions (Fig. 8). The sandstones of all localities are grey, dark-grey to greenish grey, low sorted, have psammitic structure and massive texture and lack cement. They consist of unrounded to semi-rounded clasts of mafic to felsic volcanic rocks, siliceous sedimentary rocks, quartz, plagioclase and K-feldspar submerged into a thin-grained dark matrix. The Molchanikha fine- to medium-grained, grey and dark-grey sandstones (Listvenny Fm.) consist of 0.1–0.6 mm sized lithic fragments and mineral grains: volcanic rocks (20–36%), siliceous mudstone and chert (16–28%), quartz (5–25%), plagioclase (10–19%) and K-feldspar (6–10%) (Fig. 8A, B). The magmatic rocks of lithic fragments have hyalopilitic and microlithic microstructures. The accessory minerals are zircon, titanite and mica. Several samples show secondary alteration accompanied by iron oxides and epidote.

The sandstones from Talitsa location (Talitsa Fm.) are medium-grained, dark-grey and greenish grey. The 0.1–0.7 mm clasts are lithic, magmatic rocks (24%), siliceous mudstone and chert (16%), and minerals, quartz (37%), plagioclase (17%) and K-feldspar (4%) (Fig. 8C). The hyalopilitic, intersertal and vitroporphic microstructures are well seen in the clasts of mafic to andesitic magmatic rocks. There are also rare clasts of felsic rocks (granitoides). The accessory minerals are zircon and titanite. Several samples show secondary alteration accompanied by iron oxides and epidote. In addition, we found the only outcrop of a volcanic rock, which appeared aphyric basalt (Fig. 8D).

The sandstones of the Marcheta Fm. are mostly medium- to coarse-grained, greenish grey. The clasts are volcanic rocks with abundant plagioclase laths (24–49%), sedimentary rocks (chert, siliceous mudstone; 14–24%), plagioclase (14–21%), K-feldspar (1–15%), mono- (7–17%) and polycrystalline (4–7%) quartz (Fig. 8E, F). The accessory

minerals are zircon, titanite, and mica. The secondary alteration resulted in saussuritization of plagioclase and chloritization and epidotization of mafic mineral and volcanic glass plus iron oxides. Compared to the Molchanikha and Talitsa sandstones, the Marcheta samples contain less quartz (Qt up to 22% compared with 34 and 36%, respectively) and more fragments of volcanic rocks, which also have hyalopilitic, vitroporphic and microlithic microstructures.

For a first-step classification and further tectonic discrimination, we counted at least 300 clasts of lithic and mineral fragments in 10 thin sections (Galehouse, 1971; Supplementary Table S4). According to the classification of Shutov (1967), the sandstones of the Listvenny and Talitsa formations are feldspar-quartz greywackes, whereas those of the Marcheta Fm. are mostly quartz-feldspar greywackes (Fig. 9A). Folk's classification (Folk et al., 1970), distinguishes the sandstones of all three formations as feldspatic litharenite (Fig. 9B).

6. Bulk-rock geochemistry

We characterized the chemical composition of the sandstones based on the concentrations of major oxides (27 analyses) and trace elements (20 analyses) (Supplementary Table S5). Compared to other localities, the Listvenny sandstones have higher SiO_2 (64.8–70.3 wt%), but lower TiO_2 (0.7–1.1 wt%), Al_2O_3 (11.5–14.8 wt%), Fe_2O_3 (5.2–7.0 wt%), MgO (1.8–3.0 wt%). The Marcheta sandstones show the lowest contents of SiO_2 (54.4–65.4 wt%) and notably higher TiO_2 (0.7–1.4 wt%), Al_2O_3 (14.1–18.9 wt%), Fe_2O_3 (6.7–9.6 wt%), and MgO (2.8–4.0 wt%). The chemistry of the Talitsa samples overlaps both, the Listvenny and Marcheta samples. Compared to the sandstones, the only Talitsa basalt shows the lower content of SiO_2 (48.3 wt%), similar contents of TiO_2 and Al_2O_3 (1.2 and 14.4, respectively), higher Fe_2O_3 and MgO (12.2 and = 7.9, respectively) giving $\# \text{Mg} = 56.7$, and higher $\text{CaO} = 12.0$ wt%.

The Pettijohn's classification diagram shows that the Listvenny and Talitsa samples plot in the field of greywackes. The Marcheta samples split into two groups: one is for litharenite, the second is for greywacke (Fig. 10A). To evaluate maturity and alteration, we used the index of compositional variability (ICV; Cox and Lowe, 1995) and the chemical index of alteration (CIA; Nesbitt and Young, 1982), which both are useful geochemical parameters for studying provenance and paleo-weathering of terrigenous rocks (Fig. 10B). Typically, low-weathered sediments are characterized by $\text{CIA} < 70$. The values of ICV higher than 1 indicate a low content of clay minerals, i.e., a low degree of maturity. The values of ICV in the Zalur'ya sandstones ranges from 2.0 to 2.7 indicating that the sediments are immature. The immature character of terrigenous rocks is typical, first of all, of greywackes. The values of CIA vary from 47.2 to 68.3, i.e., the sediments are relatively fresh.

In the SiO_2 versus major oxides binary plots, the compositional points form clear negative trends for TiO_2 , Al_2O_3 , MgO and Fe_2O_3 with increasing SiO_2 (Fig. 11). Such trends are typical of supra-subduction mafic to andesitic volcanic series (Tatsumi, 2005). The Talitsa basalt plots on the trend in the SiO_2 vs. Fe_2O_3 plot (Fig. 11C). In terms of trace elements, it shows $\text{Zr}/\text{Nb} = 11$, $(\text{La}/\text{Sm})_n = 3.6$, $(\text{Gd}/\text{Yb})_n = 1.8$, $(\text{La}/\text{Yb})_n = 8.8$, $(\text{Nb}/\text{Th})_{\text{pm}} = 0.2$ and $(\text{Nb}/\text{La})_{\text{pm}} = 0.2$. These features are typical of supra-subduction basalts hosted by other Pacific-type orogenic belts of the western CAOB and western Pacific (Safonova et al., 2011a,b, 2016, 2017, 2018, 2020).

The diagrams of the concentrations of rare-earth elements (REE) normalized to chondrite (Fig. 12A–C) and the multi-component diagrams of the concentrations of trace elements normalized to the primitive mantle (Fig. 12D–F) look similar to all three groups, but those for Marcheta sandstones show lower concentrations of all elements than the others. All multi-component diagrams show clear troughs at Nb–Ta ($\text{Nb}/\text{La}_{\text{pm}} = 0.2–0.6$, $\text{Nb}/\text{Th}_{\text{pm}} = 0.1–0.3$) and negative Ti anomalies that is typical of most supra-subduction magmatic series. The REE diagrams show enrichments at the light REE (LREE), but non-differentiated heavy REE (HREE). The Listvenny sandstones are more enriched in the LREE ($\Sigma \text{LREE}_{\text{av.}} = 118$), then those of the Talitsa and Marcheta localities

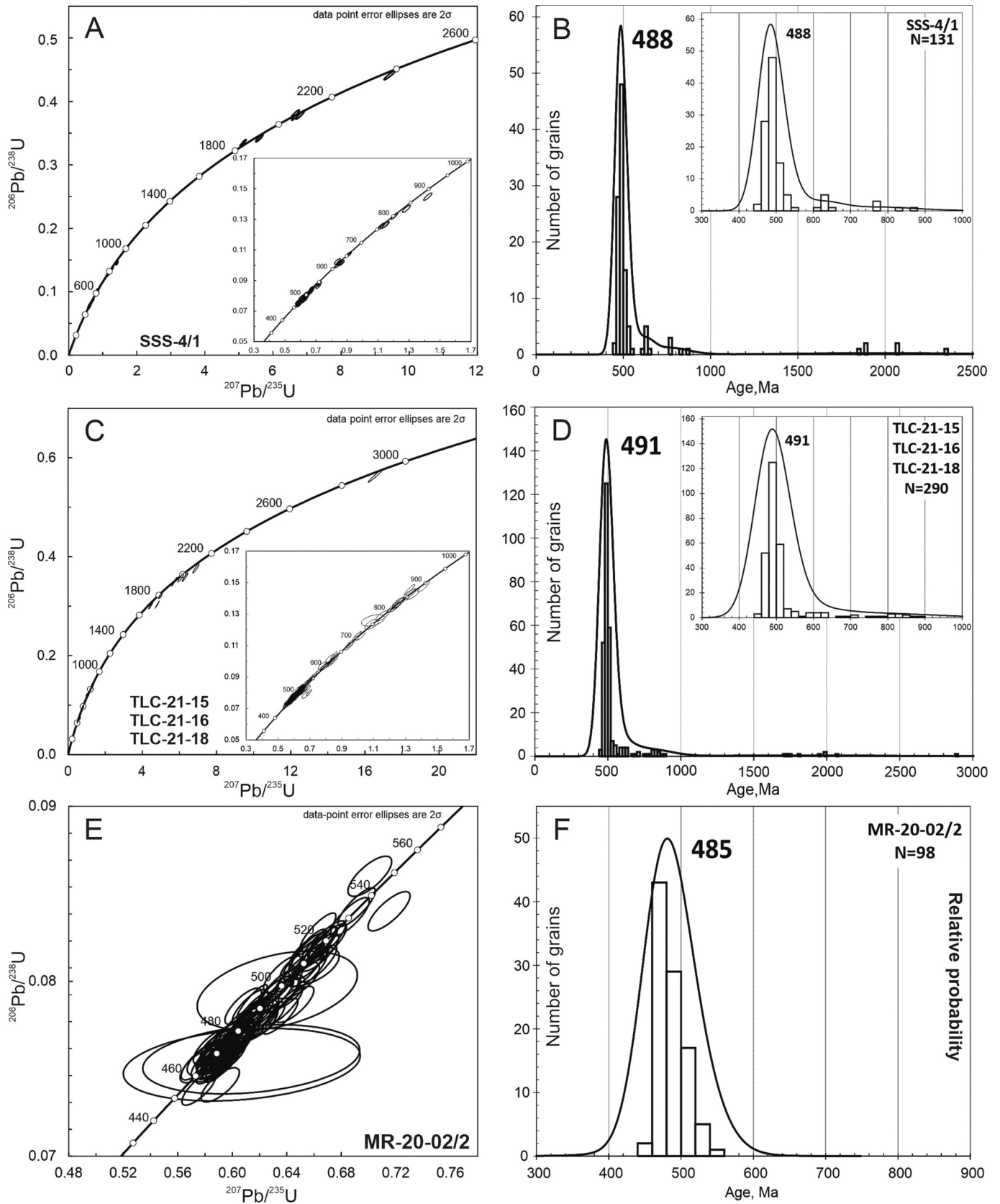


Fig. 6. U–Pb isotope data from zircons from Zalur'ya greywacke sandstones: concordia diagrams, histograms and probability curves.

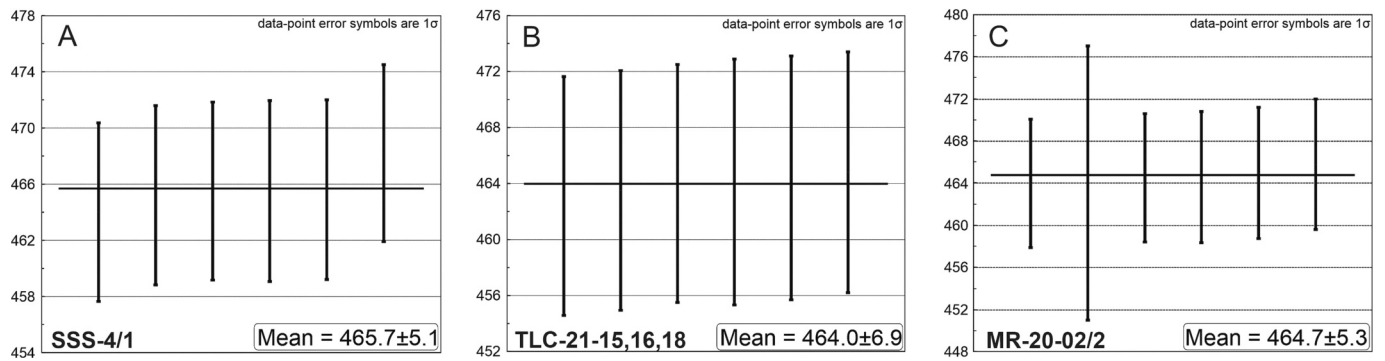


Fig. 7. Weighted averages of youngest clusters of the U—Pb zircon ages determined according to the method of (Coutts et al., 2019).

($\Sigma\text{LREE}_{\text{av.}} = 104$ and 80 , respectively). The Marcheta sandstones show a lower average content of Th (3.3 ppm) and higher Sr (533) compared to those of the Listvenny ($\text{Th}_{\text{av.}} = 5.4$ and $\text{Sr}_{\text{av.}} = 181$) and Talitsa ($\text{Th}_{\text{av.}} = 4.9$ and $\text{Sr}_{\text{av.}} = 220$) formations (Supplementary Table S5). Thus, petrographically and geochemically the sandstones under study are greywackes, first cycle immature and low-weathered sediments. The Marcheta sandstones are more mafic than those of the Listvenny and Talitsa localities. The Talitsa basalt displays the REE and multi-component patterns very similar to those of the greywackes. The overall composition of the samples in respect to both, major and trace elements, resemble those of basaltic to dacitic volcanic rocks of supra-subduction origin.

7. Sm—Nd and Lu—Hf isotope systematics

Bulk-rock Sm—Nd isotopic compositions of clastic rocks have been successfully applied by many researchers to reconstruct the modal age and juvenile or recycled character of magmatic rocks in the provenance. Here, we present first data on Sm—Nd isotope systematics from Zasur'ya greywacke sandstones (Supplementary Table S6). We chose nine most fresh samples of sandstones, three from each formation. $\text{Sm}^{147}/\text{Nd}^{144}$ and $\text{Nd}^{143}/\text{Nd}^{144}$ ratios were measured in “Geoanalyst” Center of the Institute of Geology and Geochemistry UrB RAS, Yekaterinburg, Russia (for methods see Supplementary electronic materials). Both, biostratigraphic and U—Pb detrital zircon ages, were used to calculate initial isotope ratios (see sections 3 and 4). The calculated parameters are shown in the age versus $\epsilon\text{Nd}(t)$ plot (Fig. 13A).

The Listvenny samples of the Molchanikha Locality (SSS-4/1, MOL-20-01, MOL-20-02) show the measured ratios of $^{143}\text{Nd}/^{144}\text{Nd}$ and the values of $^{147}\text{Sm}/^{144}\text{Nd}$ in the 0.512447 – 0.512456 and 0.1162 – 0.1168 ranges, respectively (Supplementary Table S6). The yielded only positive $\epsilon\text{Nd}(t)$ values (1.29 – 1.42) with Nd model ages (T_{DM2}) of 962 to 953 Ma. The Talitsa samples (TLC-21-16, 17, 18) have bit different Sm—Nd isotopes characteristics with the measured ratios of $^{143}\text{Nd}/^{144}\text{Nd}$ and the values of $^{147}\text{Sm}/^{144}\text{Nd}$ are in the ranges of 0.512449 – 0.512477 and 0.1256 – 0.1345 , respectively. The Talitsa samples yielded less positive $\epsilon\text{Nd}(t)$ values of 0.63 – 0.86 with T_{DM2} model ages of 1109 – 1051 Ma. The youngest Marcheta samples possess most juvenile isotope characteristics: the values of $^{143}\text{Nd}/^{144}\text{Nd}$ and $^{147}\text{Sm}/^{144}\text{Nd}$ span 0.512593 – 0.512683 and 0.1246 – 0.1331 , respectively, and the $\epsilon\text{Nd}(t)$ values are 3.60 – 4.83 giving the Nd model ages (T_{DM2}) of 816 to 740 Ma (Fig. 13A). Thus, the Listvenny and Talitsa sandstones show more enriched compositions and older model ages than the Marcheta samples. The Talitsa basalt yielded the measured ratios of $^{143}\text{Nd}/^{144}\text{Nd}$ and $^{147}\text{Sm}/^{144}\text{Nd}$ of 0.513220 and 0.2301 , respectively, giving the value of $\epsilon\text{Nd}(t) = 9.29$, $T_{\text{DM2}} = 640$.

Lu—Hf-in-zircon isotopes were analyzed in zircons from sandstones of all three formations (Supplementary Table S7; Fig. 13B). All analyzed zircons yielded strongly positive $\epsilon\text{Hf}(t)$ values. Fifteen zircons from sample SSS-4/1 (Listvenny Fm., Molchanikha Locality) yielded $\epsilon\text{Hf}(t)$

values of $+6.5$ to $+18.6$ (13.3 in average). The $\epsilon\text{Hf}(t)$ values of 39 zircons from the three samples of the Talitsa Fm. (TLC-21-15, 16, 18) are more variable ranging from 3.8 to 21.6 , although the mean value of 13.5 is close to that for the Listvenny Fm. The interval of the values of $\epsilon\text{Hf}(t)$ recorded in 17 zircons from Marcheta is the narrowest: from 7.5 to 19.2 (11.1 in average).

8. Age of arc magmatism and maximum deposition ages

The first U—Pb ages of detrital zircons from greywacke sandstones of the Zasur'ya AC of NW Altai are extremely important on the following reasons. First, the Zasur'ya terrane or zone represents a junction between the Gorny Altai and Rudny Altai terranes on the east and west, respectively (Fig. 2), that formed at active margins of the Siberian Continent at, respectively, the late Neoproterozoic-early Cambrian and middle Paleozoic stages of the evolution of the PAO (Buslov et al., 2000, 2001). In terms of tectonics, the Zasur'ya terrane was considered an “exotic” terrane (Buslov et al., 1999) or tectonic unit (Buslov et al., 2000) or a part of the Charysh-Terekta suture-shear zone (Glorie et al., 2011). In terms of “classic” stratigraphy, the Zasur'ya terrane was considered as a formation or suite (Iwata et al., 1997) or, later, a stratigraphic series, i. e., a group of several formations (Sennikov et al., 2003, 2011). In terms of ocean plate stratigraphy, the Zasur'ya terrane represents an accretionary complex (Safonova et al., 2011a; Safonova, 2014; Krutikova et al., in press). Second, the coeval accretionary complexes and island-arc terranes are located far to the west and east suggesting weak, if any, connection between those (e.g., Degtyarev, 2011; Konopelko et al., 2021a, 2021b; Degtyarev et al., 2021a; Safonova et al., 2020, 2022). Third, the available microfossil data provide no more or less precise age constrains on neither the lower, nor the upper boundaries of the three formations of the Zasur'ya Series (Sennikov et al., 2003). Thus, the nature of the Zasur'ya Unit has remained disputable, mostly because of the lack of up-to-date geochronological data.

We obtained U—Pb ages of detrital zircons from sandstones of all three formations of the Zasur'ya AC: Listvenny (one sample), Talitsa (three samples) and Marcheta (Fig. 6; Supplementary Fig. S4). The most wonderful feature of all age histograms is their unimodal character suggesting the derivation of sandstones from an intra-oceanic arc, i.e., an arc separated from a continental margin, a potential source of Precambrian zircons, by a back-arc basin. Continental fore-arcs, as a rule, are characterized by polymodal distributions of U—Pb zircon ages because their basements are typically built upon older rocks (Isozaki et al., 2010; Dumitru et al., 2013; Hessler and Fildani, 2015; Kirsch et al., 2016; Jackson et al., 2019). A most probable candidate for the continental block sourcing Precambrian zircons is the Altai-Mongolian terrane, which igneous formations are considered to be formed on a continental arc (Sun et al., 2008) and its clastic formations also carry Precambrian zircons (Jiang et al., 2011; Long et al., 2012). But according to another model, the Altai-Mongolian terrane represents a microcontinent (Buslov et al., 2001; Li and Poliyangsi, 2001; Yang

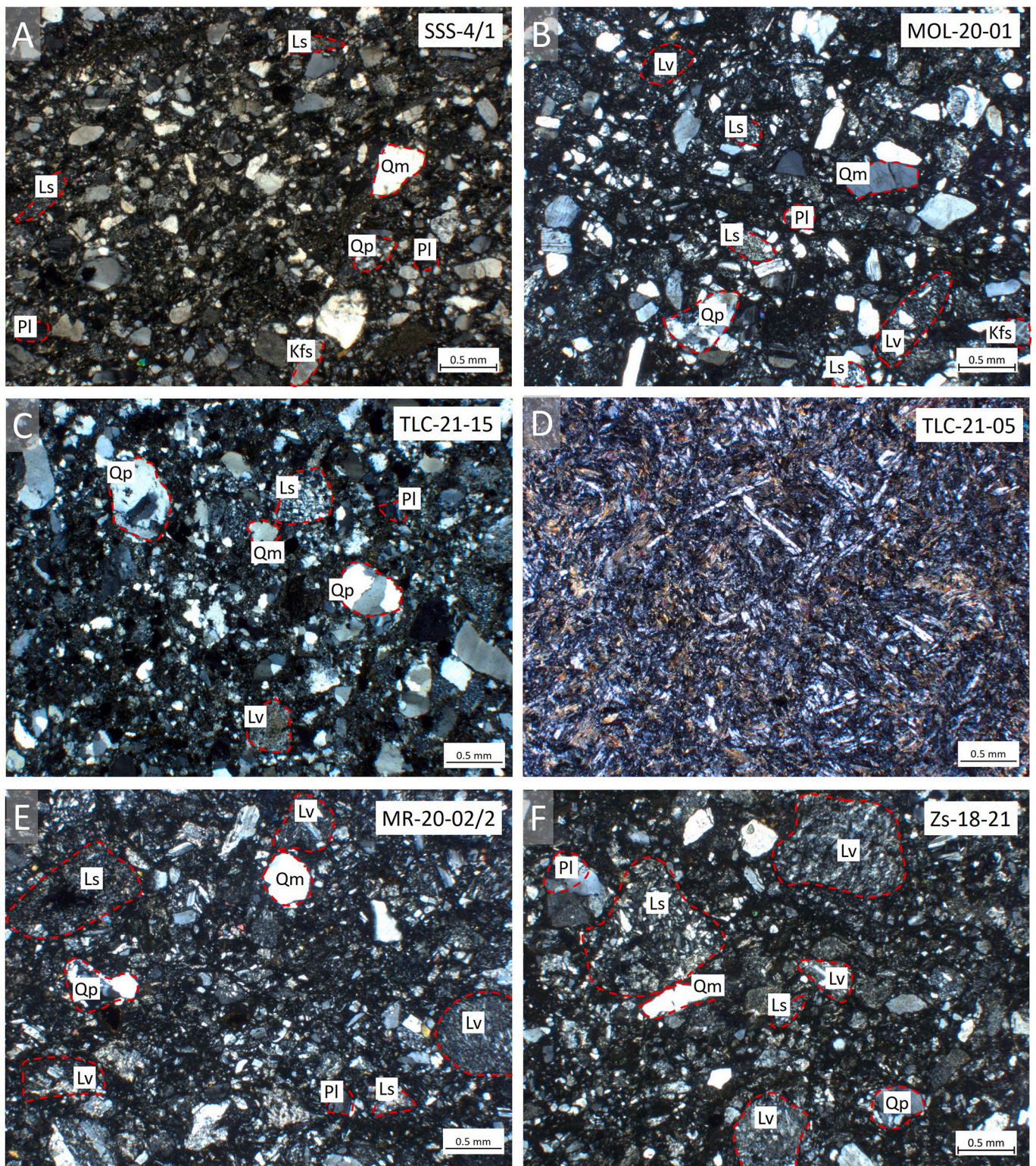


Fig. 8. Microphotographs of thin sections of sandstones and basalt: A-B – Listvenny Fm. (Molchanikha Locality); C–D – Talitsa Fm. (Talitsa Locality); E-F – Marcheta Fm. (Marcheta Locality). Qm – monocrystalline quartz, Qp – polycrystalline quartz, Pl – plagioclase, Kfs – potassium feldspar, lithic fragments of volcanic (Lv) and sedimentary (Ls) rocks.

et al., 2011). As we analyzed only magmatic zircons (Supplementary Figs. S2, S3), the obtained U–Pb ages indicate that mostly late Cambrian - Early Ordovician igneous rocks were present in the provenance. The sandstones contain many lithic fragments of volcanic rocks (Fig. 8); therefore, the provenance was highly likely a volcanic arc that

we will hereinafter refer to as “Zasur’ya arc”. The weighed averaged ages of the main peaks are 488, 491 and 485 Ma, respectively (Fig. 6), and they probably correspond to the peaks of volcanism of the Zasur’ya arc. In general, the Zasur’ya arc was active from ca. 520 to 470 Ma, i.e., about 50 Ma. Such age constrains accord well with present-day intra-oceanic

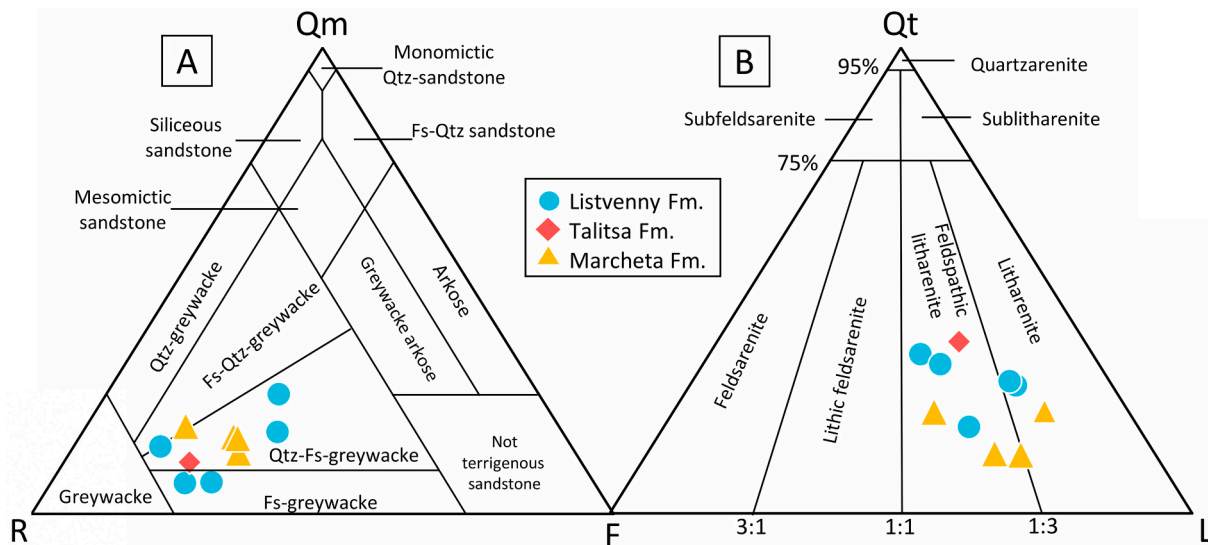


Fig. 9. Q-F-L classification diagrams for Zasut'ya sandstones: A, Shutov, 1967; B, Folk et al., 1970. Q – sum of quartz grains (Qt = Qm + Qp), F – sum of feldspar (F=Kfs + Pl), L – sum of lithic fragments (L = Ls + Lv), Qtz – quartz, Fs – feldspar.

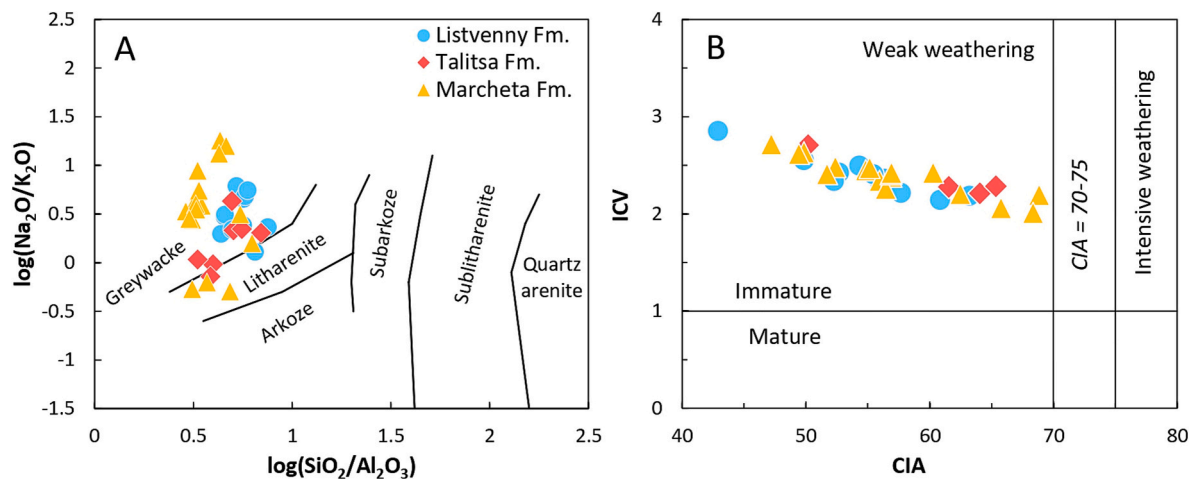


Fig. 10. A - classification diagram for sandstones of the Zasur'ya AC according to (Pettijohn et al., 1972); B - CIA vs. ICV diagram, CIA - chemical index of alteration (Nesbitt and Young, 1982), ICV – index of compositional variability (Cox and Lowe, 1995).

arcs in the western Pacific, e.g., Izu-Bonin-Mariana, Tonga, etc. (e.g., Lee et al., 1995; Falloon et al., 2008; Straub et al., 2015).

However, the age spectra of Listvenny and Talitsa sandstones show also Precambrian ages (Fig. 6; Supplementary Table S4). The portion of Precambrian ages decreases from 13% in the Listvenny sandstones to 10% in the Talitsa sandstones and, finally, to 0% in the Marcheta samples. On the other hand, the maximum deposition ages (MDA) of the three formations are similar: 466, 464 and 465 Ma (Fig. 7). Thus, according to the ages of the main peaks, the sandstones of all formations were derived from volcanic rocks of the single Zasur'ya arc. The variable amounts of Precambrian zircons suggest that clastic material for the Listvenny and Talitsa sandstones was supplied from both continental margin or continental arc (Altai-Mongolian terrane?) and intra-oceanic arc, whereas only intra-oceanic arc material was supplied to the provenance of the Marcheta sandstones.

Interestingly, the age intervals of the main peaks of zircon ages (Fig. 6) and the maximum depositional ages (Fig. 7) are similar to each other (Fig. 14), but the microfossil ages of the three formations are different (Fig. 4): late Cambrian (Listvenny Fm.), Tremadocian (Talitsa Fm.) and Tremadocian-Floian (Marcheta Fm.). By this, we conclude that the microfossil age hardly can provide robust age constraints on the

upper or lower limits of sedimentation in oceanic to fore-arc and back-arc basins, which sediments later get juxtaposed in accretionary complexes. Microfossil ages indicate the age of ocean plate from deep ocean (pelagic sediments) to shelf (hemipelagic sediments), i.e., deep-marine sedimentation, whereas the MDA inferred from zircons indicates the upper age of an accretionary complex. The microfossil ages of the deep-sea sediments of the Zasur'ya AC are different from the MDAs inferred from detrital zircons of sandstones (Figs. 4, 7). Therefore, the sandstones cannot be considered as parts of the Listvenny, Talitsa and Marcheta formations.

As the sandstones of the three formations have very close MDAs, they should be rather considered a separate formation having tectonic contacts with the sediments of the Zasur'ya AC. In principle, Japanese geologists working at late Paleozoic to Quaternary accretionary complexes of the Japanese Islands avoid distinguishing stratigraphic suites or formations at all (e.g., Kojima et al., 2000; Wakita, 2012), but consider them as units having tectonic contacts with older basements or younger superimposed formations. Basically, a combination of both microfossil and detrital zircon ages would serve a correct way for reconstructing the story of an accretionary complex from the birth of oceanic plate at mid-oceanic ridge (microfossil age) to the cessation of accretion and

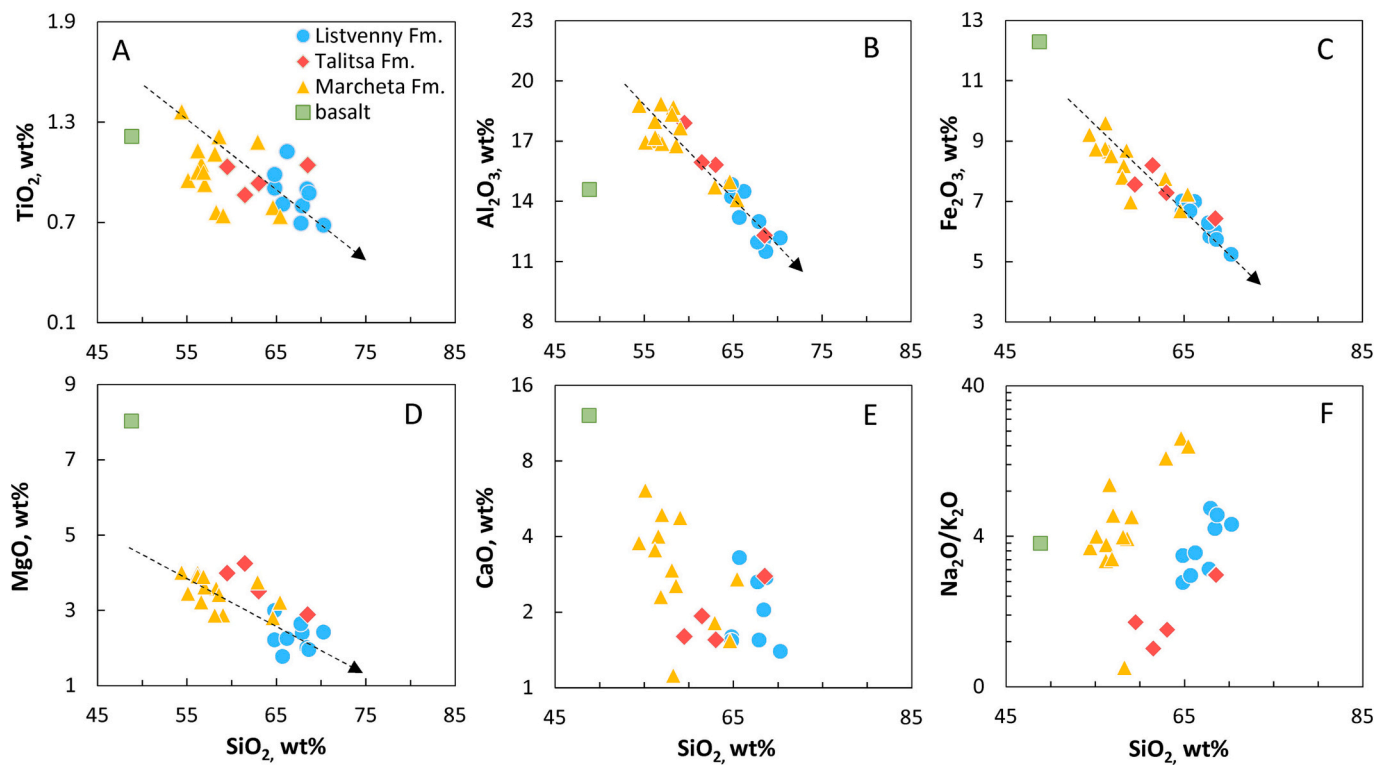


Fig. 11. Binary diagrams SiO_2 versus major oxides for sandstones and arc basalt of the Zasuk'ya AC.

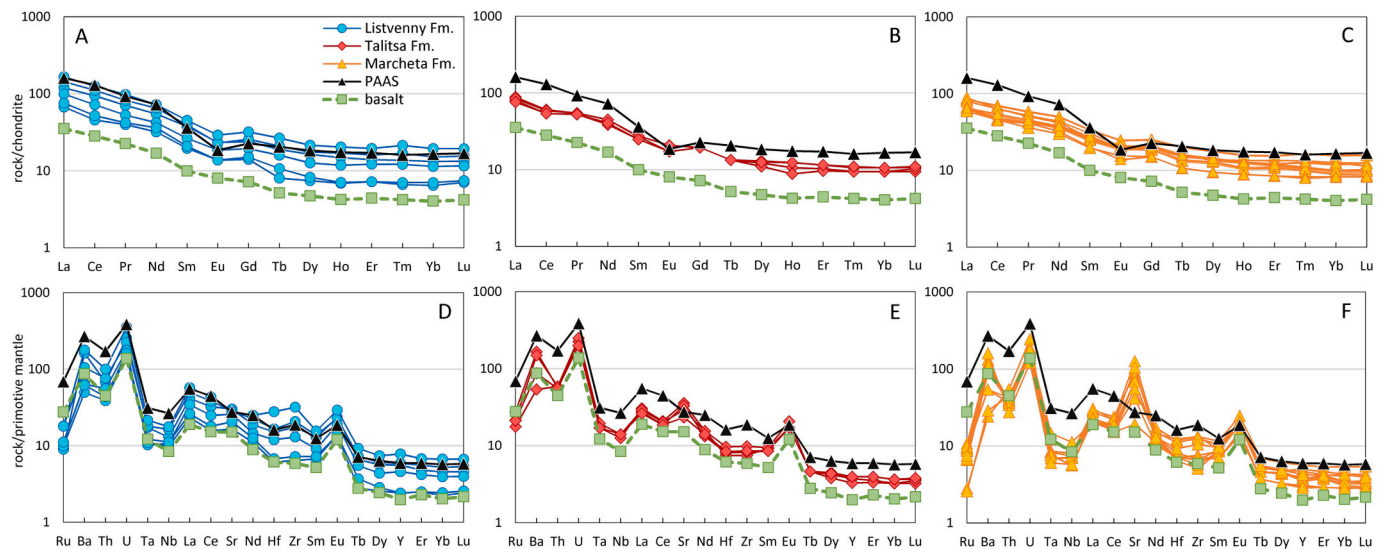


Fig. 12. Spectra of rare-earth elements (REE) normalized to chondrite (A–C) and spidergrams of trace elements normalized to primitive mantle (D–F) for sandstones and arc basalt of the Zasuk'ya AC. The compositions of chondrite and primitive mantle as in (Sun and McDonough, 1989) and that of PAAS is as in (Taylor and McLennan, 1985).

subduction (detrital zircon age).

9. Magmatic protoliths of sandstones and basins of sedimentation

All Zasuk'ya sandstones are greywackes (Figs. 8–10), i.e., they were formed through destruction of magmatic arcs. As the lithic clasts are dominated by volcanic rocks, those arcs were probably volcanic (Figs. 8, 9). The Marcheta sandstones contain less clasts of total quartz ($Q_{\text{tav}} = 17$ vol%) and more clasts of volcanic rocks ($L_{\text{vav}} = 57.2$ vol%) than those

of the Listvenny Fm. ($Q_{\text{tav}} = 27.7$, $L_{\text{vav}} = 45.4$ vol%) and Talitsa Fm. ($Q_{\text{t}} = 36.9$, $L_{\text{v}} = 41.5$ vol%) (Supplementary Table S4; Figs. 8, 9). More evidence for an arc-related origin of the sandstones under study comes from the relevant values of CIA and ICV indexes (Fig. 10), that are indicative of low degrees of weathering and fast burial on a short distance from a source. In terms of major oxides, the Listvenny and Talitsa samples are more felsic ($\text{SiO}_{2\text{av}} = 67.1$ and 63.1 wt%, respectively) than the Marcheta sandstones ($\text{SiO}_{2\text{av}} = 58.5$ wt%) (Supplementary Table S5; Fig. 11). The level of total REE of the Marcheta samples is lower than those of the Listvenny and Talitsa samples (Fig. 12). However, we can

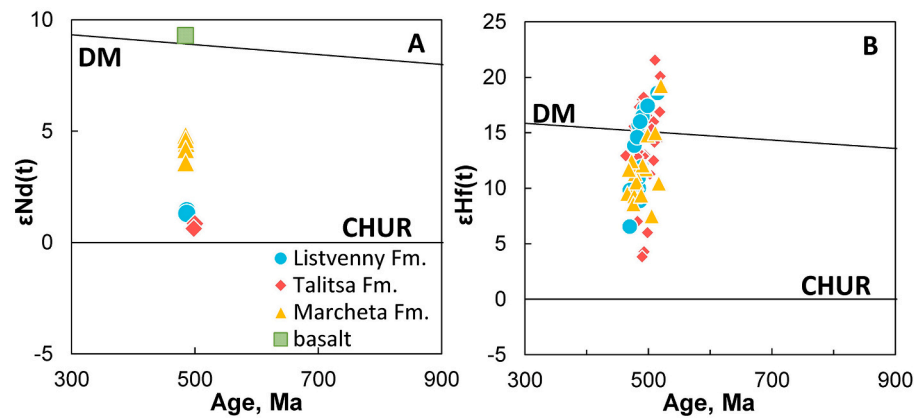


Fig. 13. Isotope data the age plots: bulk-rock Nd (A) and Hf-in-zircon (B) systematics for sandstones and arc basalt of the Zasur'ya AC. The values of $\epsilon\text{Nd}(t)$ and $\epsilon\text{Hf}(t)$ were calculated based on the U–Pb ages of detrital zircons (section 4; supplementary Table S3; Fig. 6).

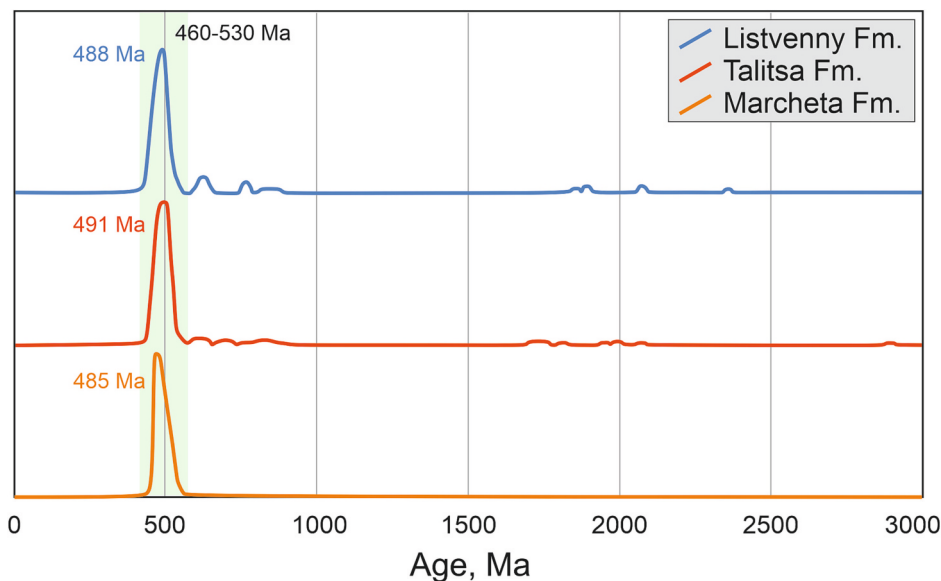


Fig. 14. Summarized probability curves of the U–Pb ages of detrital zircons from sandstones of the Listvenny (upper), Talitsa (medium) and Marcheta (lower) formations of the Zasur'ya AC illustrating the disappearance of Precambrian zircons in the younger Marcheta Fm. in the course of arc evolution and probably extension of the related back-arc basin.

recognize two groups of the Marcheta sandstones: Group 1 (hereinafter Marcheta-1) is less felsic ($\text{SiO}_2 = 55.1\text{--}58.6$ wt%) and Group 2 (hereinafter Marcheta-2) is more felsic ($\text{SiO}_2 = 64.6\text{--}65.4$ wt%), i.e., similar to the Listvenny and Talitsa samples. The Zr/Sc versus Th/Sc diagram (McLennan et al., 1993) shows that in terms of trace elements the sources of Marcheta sandstones could be also, like in terms of petrography and major oxides, compositionally between basalt and andesite, whereas the sources of the Listvenny and Talitsa sandstones were probably more felsic, i.e., between andesites and dacites (Fig. 15A). Although the Nd isotope data (Fig. 13A) indicate that the Listvenny, Talitsa and Marcheta-2 samples contain more material of recycled continental crust (e.g., continental arc) than the Marcheta-1 sandstones containing more magmatic rocks derived from juvenile mantle sources (e.g., intra-oceanic arc), the Hf isotope data show that all protoliths were juvenile (Fig. 13B). The trace-element geochemical features of the only analyzed supra-subduction basalt sampled in the Talitsa Locality (TLC-21-05, Supplementary Table S5) are almost identical to those of the most mafic sandstones (Figs. 11C, 12). More evidence for that comes from the composition of the basalt plotted on the trend in the SiO_2 vs. Fe_2O_3 binary diagram for the sandstones (Fig. 11C). The geochemical features and Nd systematics of the Talitsa basalt leave no doubts that it was

generated from a juvenile mantle source. The Talitsa basalt co-occurs with the Talitsa greywacke and therefore was a most probable magmatic protolith of those.

The geodynamic settings of sedimentation of the Zasur'ya sandstones were reconstructed using the discrimination diagrams based on petrographic counting (Supplementary Table S4) (Dickinson et al., 1983) and geochemical data (Bhatia and Crook, 1986). According to the petrographic composition, the Marcheta-1 sandstones were derived from an undissected (immature) arc (Fig. 15B), but the Marcheta-2 (more felsic) samples and those of the Listvenny and Talitsa formations were formed by erosion of a transitional and/or dissected (mature) arc. The Th-La-Sc and La/Sc vs Ti/Zr discrimination diagrams indicate that the Marcheta-1 samples were formed by erosion of an intra-oceanic arc, whereas the other sandstones by destruction of continental magmatic arc (Fig. 15C, D). These data accord well with the more mafic composition of the Marcheta-1 sandstones and more felsic compositions of the Marcheta-2, Listvenny and Talitsa samples (Supplementary Table S4; Fig. 15B). Conclusively, the petrographic and geochemical characteristics suggest that the provenances of the Listvenny, Talitsa and Marcheta-2 sandstones were dominated by andesitic to felsic volcanic rocks erupted on a dissected or mature arc. Mafic to andesitic volcanic rocks probably

dominated in the provenance of the Marcheta sandstones and were emplaced on an undissected or immature arc.

On one hand, the Listvenny and Talitsa sandstones carry more Precambrian detrital zircons (Fig. 6), have more felsic bulk rock composition (Figs. 11, 15A) and are characterized by lower $\epsilon_{Nd(t)}$ values (Fig. 13A) compared to the Marcheta sandstones (Fig. 14). On the other hand, all samples have very close ages of the main peaks of U–Pb ages (491, 488 and 485 Ma; Fig. 6) and the MDAs (ca. 464 Ma; Fig. 7) and only positive $\epsilon_{Hf(t)}$ values (Fig. 13B). The sandstones of the Listvenny, Talitsa and Marcheta fms. have slightly but not drastically different petrographic, chemical and isotope compositions. Therefore, we can propose the following scenario for the derivation and deposition of Zasuk'ya sandstones (Fig. 16). All the sandstones formed by destruction of the Zasuk'ya late Cambrian - Early Ordovician juvenile intra-oceanic arc (see also section 8 above). However, different types of materials were supplied and consequently dominated in their provenances or

participated in the process of deposition. Note that clastic material derived from an intra-oceanic arc can be deposited both in coeval back-arc and fore-arc basins. All Zasuk'ya sandstones were derived from the same protolith as they have same age and Hf-in-zircon isotope characteristics but accumulated in different basins. More felsic and clay material can be transported to a back-arc basin from an adjacent continental margin, although the intra-oceanic arc remained a main source of clastic material. So, different materials in the provenance could be derived from both sides of the back-arc basin.

The Listvenny and Talitsa sandstones were deposited in an emerging and expanding back-arc basin, at its different stages, respectively, closer and farther from the continental margin, which more felsic material and older zircons could be transported from. The typically felsic material supplied by the continental margin could be responsible for the more felsic bulk compositions of the Listvenny and Talitsa sandstones, although their major component still came from the Zasuk'ya intra-

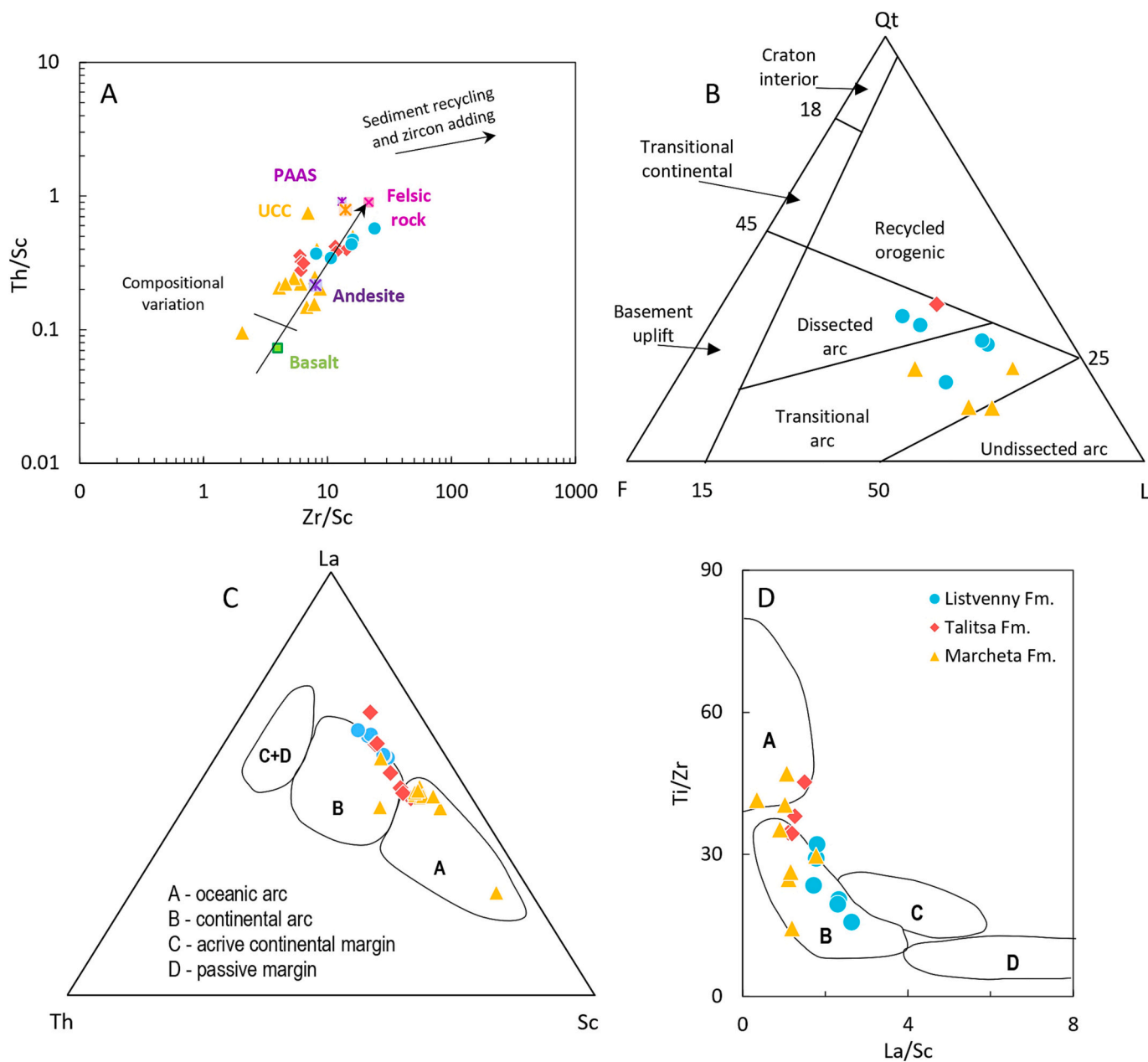


Fig. 15. Discrimination diagrams for tectonic settings in the probable provenance of sandstones of the Zasuk'ya AC: A, Zr/Sc vs. Th/Sc plot (based on McLennan et al., 1993); B, the Dickinson's ternary plot (Dickinson et al., 1983), Qm – monocrySTALLINE quartz, Qt –total quartz, F – feldspar, L – total lithic fragments; C, La/Sc vs. Th/Zr; D, La-Th-Sc (both after Bhatia and Crook, 1986).

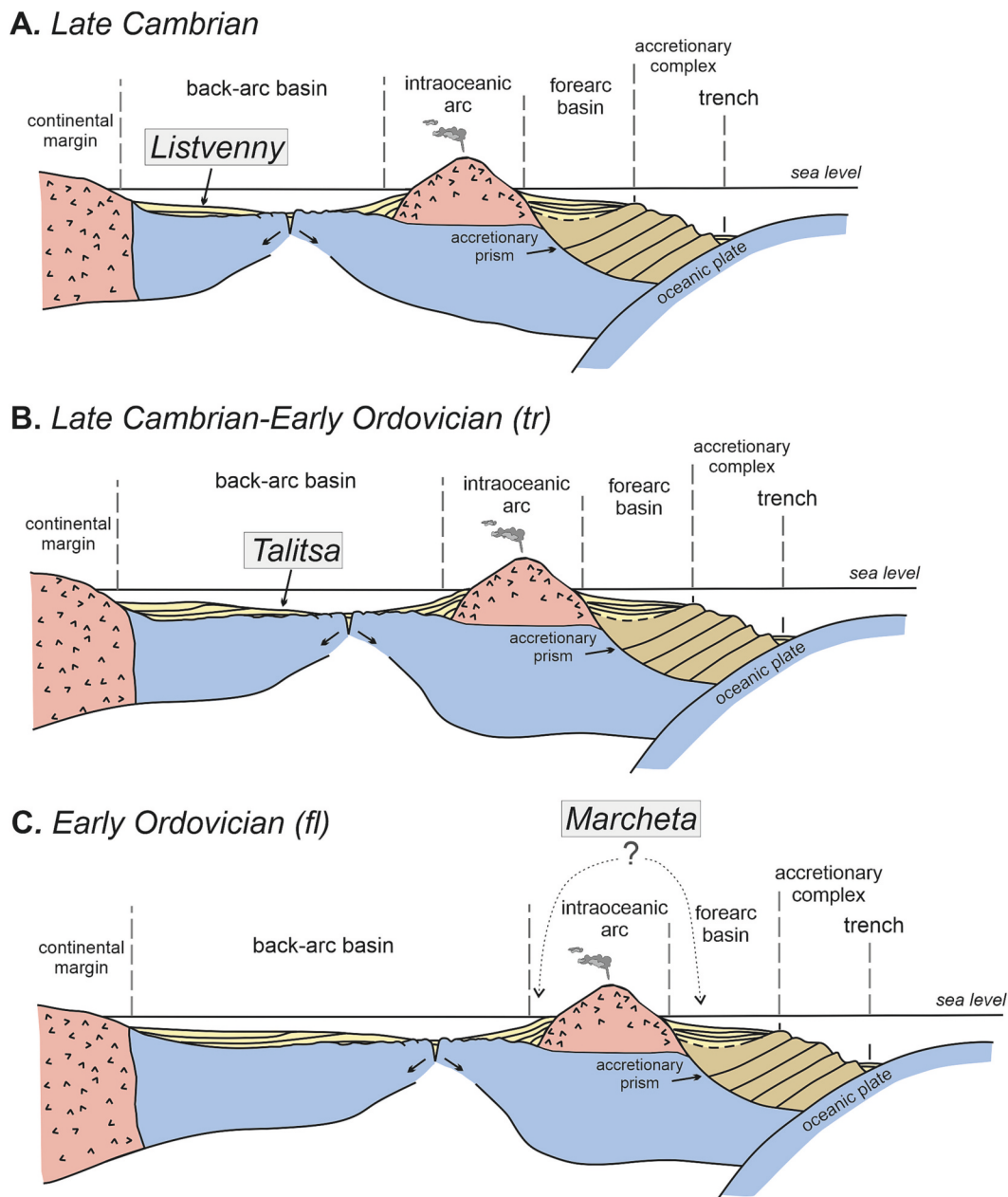


Fig. 16. A cartoon illustrating the evolution of the Zásur'ya arc and related back-arc and fore-arc sedimentation.

oceanic arc.

The Listvenny sandstones deposited on an earlier stage of back-arc rifting in an emerging back-arc basin, when more felsic /recycled material and consequently Precambrian zircons could come from the adjacent Altai-Mongolian continental block/margin (Fig. 16 A). The Talitsa and Marcheta-2 sandstones accumulated at an intermediate stage, in a larger basin, and less felsic /recycled material and consequently less Precambrian zircons were supplied from the adjacent continental block/margin (Fig. 16 B). The sandstones of the Marcheta Fm. could be accumulated either in the same back-arc basin but much closer to the arc, or in a coeval fore-arc basin, which was not reachable to recycled/felsic material (Fig. 16 C).

Thus, the clastic material of the Listvenny and Talitsa fms. was derived from felsic to andesitic magmatic rocks of both continental margin and intra-oceanic arc. The Marcheta Fm. includes clastic material derived mostly from the Zásur'ya intra-oceanic arc of mafic to felsic composition. In general, the Zásur'ya arc was located at a late Cambrian-

Early Ordovician active margin of, possibly, the Altai-Mongolian terrane, in the western part of the Paleo-Asian Ocean (Berzin et al., 1994; Buslov et al., 2001; Dobretsov et al., 2003).

10. Other late Cambrian-Early Ordovician arcs of the western CAO B

Not many late Cambrian - Early Ordovician intra-oceanic arcs have been identified in the western CAO B (Safonova et al., 2017 and references therein). All five early Paleozoic intra-oceanic subduction systems that once existed in the western PAO, are in Kazakhstan (Degtyarev, 2011; Safonova et al., 2020, 2022; Degtyarev et al., 2017, 2021a, 2021b; Gurova et al., 2022; Perfilova et al., 2022; Safonova and Perfilova, 2023): Selety-Urumbai (northern Kazakhstan), Itmurundy and Tekturmas (Central Kazakhstan), Boschekul-Chingiz and Baydaulet-Aqbastau (eastern Kazakhstan). The Boschekul-Chingiz or Chingiz-Tarbagatai arc is located in central Kazakhstan and represents the eastern wing of

the Kazakh Orocline (Degtyarev, 2011; Shen et al., 2015). The middle-late Cambrian and Ordovician intra-oceanic arcs have been diagnosed in the Itmurundy and Tekturmas accretionary complexes of central Kazakhstan as well (Safonova et al., 2020, 2022; Khassen et al., 2020; Degtyarev et al., 2021a, 2021b). There are also Ordovician arcs in southern Kazakhstan (Alexeiev et al., 2023) and West Junggar (e.g., Xu et al., 2013; Ren et al., 2014; Liu et al., 2016; Zheng et al., 2019). More specifically, there are still understudied subduction-accretionary complexes of the middle Cambrian-Ordovician age: Erqis accretionary complex in NE Junggar (Xiao et al., 2004, 2009), Kujibai ophiolitic belt in NW Junggar (Zhang et al., 2018) and Hebukesaier ophiolite in SW Junggar (Yang et al., 2019).

More to the south there is a Songkul intra-oceanic arc terrane of late Cambrian-Early Ordovician age in southern and northern Kyrgyz Tien Shan (Alexeiev et al., 2019, 2020; Konopelko et al., 2021b). However, all those arc terranes have not direct relationships with the Zasur'ya AC as located thousands of kilometers away and are separated by microcontinents and younger terrains by several suture zones (Windley et al., 2007; Xiao et al., 2010), or they are a bit older (southern Kazakhstan) or younger (central Kazakhstan). Each arc system in the western CAO is bounded by late Paleozoic extended regional faults, some of those are strike-slip faults (Fig. 1) (Buslov et al., 2004). The arc systems in other regions of the Altai Sayan folded area are all older (Dobretsov et al., 2003). No one of those arcs could serve a source area for Zasur'ya sandstones because those are first cycle sediments carrying clasts angular in shape and having immature compositions suggesting that their source(s) was/were located not far from to the basins of sedimentation (section 6). In addition, the Zasur'ya terrane is considered as exotic (Buslov et al., 1999, 2000) as bounded by two shear zones (section 3.1). Therefore, none of those arcs can be considered as potential sources of Zasur'ya sandstones. We argue that there was one more intra-oceanic arc, Zasur'ya, a real source of the sandstones under study, that was possibly located at an active margin of the Altai-Mongolian terrane and later destroyed by surface and/or subduction erosion. The only outcrop of a supra-subduction volcanic rock, the basalt TLC-21-05, represents a tiny piece of that arc survived. Thus, the Zasur'ya arc can be considered a newly recognized intra-oceanic arc, a new contribution to the juvenile crust of the CAO. The Zasur'ya arc probably was tectonically eroded and therefore disappeared as a magmatic formation from the geological record. However, its traces have been preserved in related arc-derived greywacke sandstones, which are hosted by the Zasur'ya accretionary complex of northwestern Altai.

11. Conclusions

The first geochronological, petrographic and isotope-geochemical data obtained from the sandstones of the Zasur'ya accretionary complex in northwestern Altai (Listvenny, Talitsa and Marcheta formations) as combined with the available geological and microfossil data allowed us to conclude about the following. The sandstones under study are associated with oceanic basalts and deep-sea sediments, pelagic (ribbon chert) and hemipelagic (siliceous mudstone, siltstone, shale). The distribution patterns of the U—Pb ages of detrital zircons are all unimodal suggesting their derivation from a late Cambrian - Early Ordovician intra-oceanic arc. The MDA of the sandstones of all three formations is ca. 464 Ma and it disagrees with the ages constrained by microfossils. Therefore, the stratigraphic subdivisions of the study area require revision.

Petrographically and geochemically, all the sandstones are greywackes, but the bulk-rock compositions of the Listvenny and Talitsa samples are more felsic than those of the Marcheta sandstones. The Nd isotope data indicate that the Listvenny and Talitsa samples contain more material of recycled continental crust than the Marcheta sandstones that were derived from magmatic rocks with juvenile isotope characteristics. The Hf isotope data show that the magmatic protoliths of the sandstones of all three formations of the Zasur'ya AC were derived

from juvenile mantle sources and emplaced at an intra-oceanic arc.

In terms of provenance, the clastic materials of the Listvenny and Talitsa sandstones were supplied from both a continental margin and intra-oceanic arc, whereas the provenance of Marcheta sandstones was dominated by only intra-oceanic arc igneous rocks.

The geological position in the Zasur'ya AC, the greywacke nature of the sandstones, the unimodal distributions of U—Pb detrital zircon ages, and the positive $\epsilon\text{Hf}(t)$ (+4.3 to +20.1), and $\epsilon\text{Nd}(t)$ (+0.6 to +4.8) inevitably prove that the sandstones of all three formations were derived from volcanic rocks of a single intra-oceanic arc that was active from ca. 520 to 470 Ma, i.e., about 50 Ma. That arc possibly existed at an active margin of the Altai-Mongolian terrane and definitely contributed to the early Paleozoic juvenile crustal growth of the western CAO. Later, the Zasur'ya arc was probably fully destroyed by surface and/or subduction erosion.

Supplementary data to this article can be found online at <https://doi.org/10.1016/j.earscirev.2023.104648>.

Declaration of Competing Interest

The authors declare that they have no known competing financial interests or personal relationships that could have appeared to influence the work reported in this paper.

Data availability

No data was used for the research described in the article.

Acknowledgments

We thank Prof. W. Xiao for inviting us to contribute to the "Altaid" Special Issue. More thanks go to Dr. Nikolai Sennikov for fruitful discussions about the Zasur'ya Series, to Drs. P. Kotler, I. Savinskiy, B. Gan and R. Mamlin for joint field works and to A. Gurova for help with figure drawing and to N. Soloshenko for help with Nd analyses (Geoanalytical Center, IGG UrB RAS, Yekaterinburg). The study was supported by the Russian Science Foundation (#21-77-20022; geochronology, stratigraphy, geochemistry), Fundamental Research Funds for the Central Universities of China (2682023CX016, geodynamic implications, paper preparation), and Ministry of Science and Higher Education of Russia, State Assignment Projects (122041400044-2, FSUS-2020-0039) (petrography, geodynamic implications, paper preparation).

References

- Alexeiev, D.V., Kröner, A., Kovach, V.P., Tretyakov, A.A., Rojas-Agramonte, Y., Degtyarev, K.E., Mikolaichuk, A.V., Wong, J., Kiselev, V.V., 2019. Evolution of Cambrian and early Ordovician arcs in the Kyrgyz North Tianshan: Insights from U-Pb zircon ages and geochemical data. *Gondwana Res.* 66, 93–115.
- Alexeiev, D.V., Biske, G.S., Kröner, A., Tretyakov, A.A., Kovach, V.P., Rojas-Agramonte, Y., 2020. Ediacaran, early Ordovician and early Silurian arcs in the south Tianshan orogen of Kyrgyzstan. *J. Asian Earth Sci.* 190, 104194.
- Alexeiev, D.V., Khudoley, A.K., DuFrane, S.A., Glorie, S., Vishnevskaya, I.A., Semiletkin, S.A., Letnikova, E.F., 2023. Early Neoproterozoic fore-arc basin strata of the Malyi Karatau Range (South Kazakhstan): Depositional ages, provenance and implications for reconstructions of Precambrian continents. *Gondwana Res.* 119, 313–340.
- Berzin, N.A., Coleman, R.G., Dobretsov, N.L., Zonenshain, L.P., Xiao, X., Chang, E.Z., 1994. Geodynamic map of the western part of the Paleozoic Ocean. *Russ. Geol. Geophys.* 35, 8–28.
- Bhatia, M.R., Crook, K.A.W., 1986. Trace elements characteristics of graywackes and tectonic setting discrimination of sedimentary basins. *Contrib. Mineral. Petrol.* 92, 181–193.
- Biske, Y.S., Alexeiev, D.V., Ershova, V.B., Priyatkina, N.S., DuFrane, S.A., Khudoley, A.K., 2019. Detrital zircon U-Pb geochronology of middle Paleozoic sandstones from the South Tianshan (Kyrgyzstan): Implications for provenance and tectonic evolution of the Turkestan Ocean. *Gondwana Res.* 75, 97–117.
- Burg, J.-P., 2018. Geology of the onshore Makran accretionary wedge: Synthesis and tectonic interpretation. *Earth Sci. Rev.* 185, 1210–1231.
- Buslov, M.M., 2011. Tectonics and geodynamics of the Central Asian fold belt: the role of late Paleozoic large-amplitude strike-slip faults. *Russ. Geol. Geophys.* 52, 52–71.

- Buslov, M.M., Safonova, I.Y., 2010. Guide-Book for the Post-Symposium Excursion of Siberian Continent Margins, Altai-Mongolian Gondwana-derived Terrane and Their Separating Suture-shear Zone, Novosibirsk, Russia, 74p.
- Buslov, M.M., Safonova, I.Yu., Bobrov, V.A., 1999. Exotic terrain of late Cambrian-early Ordovician oceanic crust in the north-western Gornyi Altai (Zasurin formation): Structural position and geochemistry. *Dokl. Earth Sci.* 368, 650–654.
- Buslov, M.M., Fujiwara, I., Safonova, I.Yu., Okada, Sh., Semakov, N.N., 2000. The junction zone of the Gornyi Altai and Rudny Altai terrains: Structure and evolution. *Russ. Geol. Geophys.* 41, 383–397.
- Buslov, M.M., Saphonova, I.Yu., Watanabe, T., Obut, O.T., Fujiwara, Y., Iwata, K., Semakov, N.N., Sugai, Y., Smirnova, L.V., Kazansky, A.Yu., 2001. Evolution of the Paleo-Asian Ocean (Altai–Sayan Region, Central Asia) and collision of possible Gondwana-derived terranes with the southern marginal part of the Siberian continent. *Geosci. J.* 5, 203–224.
- Buslov, M.M., Watanabe, T., Saphonova, I.Yu., Iwata, K., Travin, A.V., 2002. Vendian - Cambrian island-arc system of the Siberian continent in Gornyi Altai (Russia, Central Asia). *Gondwana Res.* 5, 781–800.
- Buslov, M.M., Watanabe, T., Fujiwara, Y., Iwata, K., Smirnova, L.V., Safonova, I.Yu., Semakov, N.N., Kiryanova, A.P., 2004. Late Paleozoic faults of the Altai region, Central Asia: tectonic pattern and model of formation. *J. Asian Earth Sci.* 23, 655–671.
- Clift, P.D., Vannucchi, P., 2004. Controls on tectonic accretion versus erosion in subduction zones: implications for the origin and recycling of the continental crust. *Rev. Geophys.* 42, RG2001.
- Coutts, D.S., Matthews, W.A., Hubbard, S.M., 2019. Assessment of widely used methods to derive depositional ages from detrital zircon populations. *Geosci. Front.* 10, 1421–1435.
- Cox, R., Lowe, D.R., 1995. A conceptual review of regional-scale controls on the composition of clastic sediment and the co-evolution of continental blocks and their sedimentary cover. *J. Sediment. Res.* 1, 1–12.
- Cunningham, W.D., Windley, B.F., Dorjnamjaa, D., Badamgarov, G., Saandar, M., 1996. Late Cenozoic transpression in South-Western Mongolia and the Gobi Altai-Tien Shan connection. *Earth Planet. Sci. Lett.* 140, 67–82.
- Defant, M.J., Drummond, M.S., 1990. Derivation of some modern arc magmas by melting of young subducted lithosphere. *Nature* 347, 662–665.
- Degtyarev, K.E., 2011. Tectonic evolution of early Paleozoic island-arc systems and continental crust formation in the caledonides of Kazakhstan and the North Tien Shan. *Geotectonics* 45, 23–50.
- Degtyarev, K.E., Tolmacheva, T.Y., Tretyakov, A.A., Kotov, A.B., Yakubchuk, A.S., Salnikova, E.B., Wang, K.-L., 2017. Polychronous formation of the ophiolite association in the Tekturmas zone of Central Kazakhstan inferred from geochronological and biostratigraphic data. *Dokl. Earth Sci.* 472, 26–30.
- Degtyarev, K.E., Luchitskaya, M.V., Tretyakov, A.A., Pilitsyna, A.V., Yakubchuk, A.S., 2021a. Early Paleozoic suprasubduction complexes of the North Balkhash ophiolite zone (Central Kazakhstan): Geochronology, geochemistry and implications for tectonic evolution of the Junggar-Balkhash Ocean. *Lithos* 380–381, 105818.
- Degtyarev, K., Yakubchuk, A.S., Luchitskaya, M.V., Tolmacheva, T.Yu., Skoblenko, A.V., Tretyakov, A.A., 2021b. Ordovician supra-subduction, oceanic and within-plate ocean island complexes in the Tekturmas ophiolite zone (Central Kazakhstan): age, geochemistry and tectonic implications. *Int. Geol. Rev.* <https://doi.org/10.1080/00206814.2021.1969691>.
- Dickinson, W.R., Beard, L.S., Brakenridge, G.R., Erjavec, J.L., Ferguson, R.C., Inman, K. F., Knepp, R.A., Lindberg, F.A., Ryberg, P.T., 1983. Provenance of north American Phanerozoic sandstones in relation to tectonic setting. *Geol. Soc. Am. Bull.* 94, 222–235.
- Didenko, A.N., Mossakovskii, A.A., Pecherskii, D.M., Ruzhentsev, S.V., Samygin, S.G., Kheraskova, T.N., 1994. Geodynamics of Paleozoic oceans of Central Asia. *Russ. Geol. Geophys.* 35, 56–78.
- Dobretsov, N.L., Buslov, M.M., Vernikovskiy, V.A., 2003. Neoproterozoic to early Ordovician evolution of the Paleo-Asian Ocean: implications to the break-up of Rodinia. *Gondwana Res.* 6, 143–159.
- Dumitru, T.A., Ernst, W.G., Wright, J.E., Wooden, J.L., Wells, R.E., Farmer, L.P., Graham, S.A., 2013. Eocene extension in Idaho generated massive sediment floods into the Franciscan trench and into the Tye, Great Valley, and Green River basins. *Geology* 41, 187–190.
- Falloon, T.J., Danyushevsky, L.V., Crawford, A.J., Meffre, S., Woodhead, J.D., Bloomer, S.H., 2008. Boninites and adakites from the northern termination of the Tonga Trench: implications for adakite petrogenesis. *J. Petrol.* 49, 697–715.
- Folk, R.L., Andrews, P.B., Lewis, D.W., 1970. Detrital sedimentary rock classification and nomenclature for use in New Zealand. *New Zealand J. Geol. Geophys.* 13, 937–968.
- Galehouse, J.S., 1971. Sedimentation analysis. In: Carver, R. (Ed.), *Procedures in Sedimentary Petrology*. Wiley–Interscience, London, pp. 69–94.
- Ganbat, A., Tsujimori, T., Miao, L., Safonova, I., Pastor-Galán, D., Anaad, C., Baatar, M., Aoki, S., Aoki, K., Savinskiy, I., 2021. Late Paleozoic–Early Mesozoic granitoids in the Khangay–Khentey basin, Central Mongolia: Implication for the tectonic evolution of the Mongol–Okhotsk Ocean margin. *Lithos* 404–405, 9842R2.
- Gazel, E., Hayes, J., Kaj, H., Yagodinski, G., 2015. Continental crust generated in oceanic arcs. *Nat. Geosci.* 8, 321–327.
- Glorie, S., De Grave, J., Buslov, M.M., Zhimulev, F.I., Izmer, A., Elburg, M.A., Ryabinin, A.B., Van-doorne, W., Vanhaeke, F., Van den Haute, P., 2011. Formation and Paleozoic evolution of the Gornyi-Altai-Mongolia suture zone (Siberia): zircon U/Pb constraints on its igneous record. *Gondwana Res.* 20, 465–484.
- Gurova, A.V., Safonova, I.Yu., Savinskiy, I.A., Antonyuk, R.M., Orynbek, T.Zh., 2022. Magmatic Rocks of the Tekturmass Accretionary complex, Central Kazakhstan: Geological Position and Geodynamic Settings of Formation. *Geodyn. Tectonophys.* 13, 0673. <https://doi.org/10.5800/GT-2022-13-5-0673>.
- Hanchar, J.M., Hoskin, P.W.O., 2003. Zircon. *Rev. Mineral. Geochem.* 53, 500 p.
- Hessler, A.M., Fildani, A., 2015. Andean forearc dynamics as recorded by detrital zircon from the Eocene Talara Basin, Northwest Peru. *J. Sediment. Res.* 85, 646–659.
- Hu, W., Li, P., Sun, M., Safonova, I., Jiang, Y., Yuan, C., Kotler, P., 2022. Provenance of late Paleozoic sedimentary rocks in eastern Kazakhstan: Implications for the collision of the Siberian margin with the Kazakhstan collage. *J. Asian Earth Sci.* 232, 104978.
- Isozaki, Y., Maruyama, S., Fukuoka, F., 1990. Accreted oceanic materials in Japan. *Tectonophysics* 181, 179–205.
- Isozaki, Y., Aoki, K., Nakama, T., Yanai, S., 2010. New insight into a subduction-related orogeny: Re-appraisal on geotectonic framework and evolution of the Japanese Islands. *Gondwana Res.* 18, 82–105.
- Iwata, K., Sennikov, N.V., Buslov, M.M., Obut, O.T., Shokalskii, S.P., Kuznetsov, S.A., Ermikov, V.D., 1997. Latter Cambrian-early Ordovician age of the Zalur'ia Basalt-Siliceous-Terrigenous formation (northwestern part of Gornyi Altai). *Russ. Geol. Geophys.* 38, 1427–1444.
- Jackson, L.J., Horton, B.K., Vallejo, C., 2019. Detrital zircon U-Pb geochronology of modern Andean rivers in Ecuador: Fingerprinting tectonic provinces and assessing downstream propagation of provenance signals. *Geosphere* 15, 1943–1957.
- Jiang, Y., Sun, M., Zhao, G., Yuan, C., Xiao, W., Xia, X., Long, X., Wu, F., 2011. Precambrian detrital zircons in the early Paleozoic Chinese Altai: their provenance and implications for the crustal growth of Central Asia. *Precambrian Res.* 189, 140–154.
- Kelemen, P.B., Shimizu, N., Salters, V.J.M., 1995. Extraction of mid-ocean-ridge basalt from the upwelling mantle by focused flow of melt in dunite channels. *Nature* 375, 747–753.
- Khasen, B.P., Safonova, I.Y., Yermolov, P.V., Antonyuk, R.M., Gurova, A.V., Obut, O.T., Perfilova, A.A., Savinskiy, I.A., Tsujimori, T., 2020. The Tekturmas ophiolite belt of Central Kazakhstan: Geology, magmatism, and tectonics. *Geol. J.* 55, 2363–2382.
- Kirsch, M., Paterson, S.R., Wobbe, F., Ardila, A.M.M., Clausen, B.L., Alasino, P.H., 2016. Temporal histories of Cordilleran continental arcs: Testing models for magmatic periodicity. *Am. Mineral.* 101, 2133–2154.
- Kojima, S., Kemkin, I.V., Kametaka, M., Ando, A., 2000. A correlation of accretionary complexes of southern Sikhote-Alin of Russia and the inner zone of southern Japan. *Geosci. J.* 4, 175–185.
- Komiya, T., Maruyama, S., Masuda, T., Nohda, S., Hayashi, M., Okamoto, K., 1999. Plate Tectonics at 3.8–3.7 Ga. Field evidence from the Isua accretionary complex, Southern West Greenland. *J. Geol.* 107, 515–554.
- Konopelko, D., Safonova, I., Perfilova, A., Biske, Y., Mirkamalov, R., Divaev, F., Kotler, P., Obut, O., Wang, B., Sun, M., Soloshenko, N., 2021a. Detrital zircon U-Pb-Hf isotopes and whole-rock geochemistry of Eidiacaran - Silurian clastic sediments of the Uzbek Tienshan: sources and tectonic implications. *Int. Geol. Rev.* 64, 3005–3027.
- Konopelko, D., Seltmann, R., Dolgoplova, A., Safonova, I., Glorie, S., De Grave, J., Sun, M., 2021b. Adakite-like granitoids of Songkultau: a relic of juvenile Cambrian arc in Kyrgyz Tien Shan. *Geosci. Front.* 12, 147–160.
- Kovalenko, V.I., Yarmolyuk, V.V., Kovach, V.P., Kotov, A.B., Kozakov, I.K., Salnikova, E. B., Larin, A.M., 2004. Isotope provinces, mechanisms of generation and sources of the continental crust in the Central Asian mobile belt: geological and isotopic evidence. *J. Asian Earth Sci.* 23, 605–627.
- Kröner, A., Kovach, V., Belousova, E., Hegner, E., Armstrong, R., Dolgoplova, A., Seltmann, R., Alexeiev, D.V., Hofmann, J.E., Wong, J., Sun, M., Cai, K., Wang, T., Tong, Y., Wilde, S.A., Degtyarev, K.E., Rytisk, E., 2014. Reassessment of continental growth during the accretionary history of the Central Asian Orogenic Belt. *Gondwana Res.* 25, 103–125.
- Kröner, A., Kovach, V., Alexeiev, D., Wang, K.-L., Wong, J., Degtyarev, K., Kozakov, I., 2017. No excessive crustal growth in the Central Asian Orogenic Belt: further evidence from field relationships and isotopic data. *Gondwana Res.* 50, 135–166.
- Kruk, N.N., Kuibida, Y.V., Shokalsky, S.P., Kiselev, V.I., Gusev, N.I., 2018. Late Cambrian – early Ordovician turbidites of the Gornyi Altai (Russia): compositions, sources, deposition settings, and tectonic implications. *J. Asian Earth Sci.* 159, 209–232.
- Krutikova, A.K., Safonova, I.Yu., Obut, O.T., Perfilova, A.A., Savinskiy, I.A., Sennikov, N. V., Gan, B., n.d. (in press). Geological position and composition of sandstones of the Listvenny and Marcheta Formations of the Zalur'ya Series. *Gornyi Altai. Lithosphere*.
- Kusky, T., Windley, B., Safonova, I., Wakita, K., Wakabayashi, J., Polat, A., Santosh, M., 2013. Recognition of Ocean Plate Stratigraphy in accretionary orogens through Earth history: a record of 3.8 billion years of sea floor spreading, subduction, and accretion. *Gondwana Res.* 24, 501–547.
- Lee, J.M., Stern, R.J., Bloomer, S.H., 1995. Forty million years of magmatic evolution in the Mariana arc: the tephra record. *J. Geophys. Res.* 100, 17671–17687.
- Li, T.D., Poliyangsi, B.H., 2001. Tectonics and crustal evolution of Altai in China and Kazakhstan. *Xinjiang Geol.* 19, 27–32. (in Chinese).
- Li, D.P., Li, X.L., Zhou, X.K., Wang, X.L., Li, W., Gao, X.P., Du, S.X., Dai, X.Y., Liu, Y.Q., 2007. Discovery of a Permian paleo-seamount in the western segment of the Bayan Har Mountains, China and its significance. *Geol. Bull. China* 26, 996–1002 (in Chinese with English abstract).
- Liu, B., Han, B., Xu, Z., Ren, R., Zhang, J., Zhou, J., Su, L., Li, Q., 2016. The Cambrian initiation of intra-oceanic subduction in the southern Paleo-Asian Ocean: further evidence from the Barleik subduction related metamorphic complex in the West Junggar region, NW China. *J. Asian Earth Sci.* 123, 1–21.
- Long, X., Yuan, C., Sun, M., Safonova, I., Xiao, W., Wang, Y., 2012. Geochemistry and U-Pb detrital zircon dating of Paleozoic graywackes in East Junggar, NW China: Insights into subduction-accretion processes in the southern Central Asian Orogenic Belt. *Gondwana Res.* 21, 637–653.
- Maruyama, S., Kawai, T., Windley, B.F., 2010. Ocean plate stratigraphy and its imbrication in an accretionary orogen: the Mona complex, Anglesey-Lleyn, Wales, UK. *Geol. Soc. London Spec. Publ.* 338, 55–75.

- McLennan, S.M., Hemming, S., McDaniel, D.K., Hanson, G.N., 1993. Geochemical approaches to sedimentation, provenance and tectonics. In: Johnsson, M.J., Basu, A. (Eds.), *Processes Controlling the Composition of Clastic Sediments*, Geol. Soc. Am. Spec. Pap., vol. 28, pp. 21–40.
- Nesbitt, H.W., Young, G.M., 1982. Early Proterozoic climates and plate motions inferred from major element chemistry of lutites. *Nature* 299, 715–717.
- Obut, O.T., 2023. Early Paleozoic plankton evolution in the Paleo-Asian Ocean: insights from new and reviewed fossil records from the Gorny Altai, West Siberia. *Paleont. Res.* 27, 3–13.
- Perfilova, A.A., Safonova, I.Yu., Degtyarev, K.E., Savinsky, I.A., Kotler, P.D., Khassen, B. P., 2022. Composition and sources of Silurian terrigenous rocks at the periphery of the Tekurmas ophiolite zone (Central Kazakhstan). *Dokl. Earth Sci.* 505, 416–421.
- Pettijohn, F.J., Potter, P.E., Siever, R., 1972. *Sand and Sandstones*. Springer-Verlag, New York, 618 p.
- Ren, R., Han, B., Hu, Z., Zhou, Y., Liu, B., Zhang, L., Chen, J., Su, L., Li, J., Li, X., Li, Q., 2014. When did the subduction first initiate in the southern Paleo-Asian Ocean: new constraints from a Cambrian intra-oceanic arc system in West Junggar, NW China. *Earth Planet. Sci. Lett.* 388, 222–236.
- Safonova, I.Y., 2009. Intraplate magmatism and oceanic plate stratigraphy of the Paleo-Asian and Paleo-Pacific Oceans from 600 to 140 Ma. *Ore Geol. Rev.* 35, 137–154.
- Safonova, I., 2014. The Russian-Kazakh Altai orogen: an overview and main debatable issues. *Geosci. Front.* 5, 537–552.
- Safonova, I., 2017. Juvenile versus recycled crust in the Central Asian Orogenic Belt: Implications from ocean plate stratigraphy, blueschist belts and intra-oceanic arcs. *Gondwana Res.* 47, 6–27.
- Safonova, I., Perfilova, A., 2023. Survived and disappeared intra-oceanic arcs of the Paleo-Asian Ocean: evidence from Kazakhstan. *National Science Review. Earth Sci.* 10 <https://doi.org/10.1093/nsr/nwac215>.
- Safonova, I., Santosh, M., 2014. Accretionary complexes in the Asia-Pacific region: tracing archives of ocean plate stratigraphy and tracking mantle plumes. *Gondwana Res.* 25, 126–158.
- Safonova, I.Y., Buslov, M.M., Iwata, K., Kokh, D.A., 2004. Fragments of Vendian-early Carboniferous oceanic crust of the Paleo-Asian Ocean in foldbelts of the Altai-Sayan region of Central Asia: geochemistry, biostratigraphy and structural setting. *Gondwana Res.* 7, 771–790.
- Safonova, I.Yu., Simonov, V.A., Buslov, M.M., Ota, T., Maruyama, Sh., 2008. Neoproterozoic basalts of the Paleo-Asian Ocean (Kurai accretion zone, Gorny Altai, Russia): geochemistry, petrogenesis, geodynamics. *Russ. Geol. Geophys.* 49, 254–271.
- Safonova, I.Y., Sennikov, N.V., Komiya, T., Bychkova, Y.V., Kurganskaya, E.V., 2011a. Geochemical diversity in oceanic basalts hosted by the Zsaur'ya accretionary complex, NW Russian Altai, Central Asia: Implications from trace elements and Nd isotopes. *J. Asian Earth Sci.* 42, 191–207.
- Safonova, I.Yu., Buslov, M.M., Simonov, V.A., Izokh, A.E., Komiya, T., Kurganskaya, E. V., Ohno, T., 2011b. Geochemistry, petrogenesis and geodynamic origin of basalts from the Katun accretionary complex of Gorny Altai, south-western Siberia. *Russ. Geol. Geophys.* 52, 421–442.
- Safonova, I., Maruyama, S., Kojima, S., Komiya, T., Krivonogov, S., Koshida, K., 2016. Recognizing OIB and MORB in accretionary complexes: a new approach based on ocean plate stratigraphy, petrology, and geochemistry. *Gondwana Res.* 33, 92–114.
- Safonova, I., Kotlyarov, A., Krivonogov, S., Xiao, W., 2017. Intra-oceanic arcs of the Paleo-Asian Ocean. *Gondwana Res.* 50, 167–194.
- Safonova, I., Komiya, T., Romer, R., Simonov, V., Seltmann, R., Rudnev, S., Yamamoto, Sh., Sun, M., 2018. Supra-subduction igneous formations of the Char ophiolite belt, East Kazakhstan. *Gondwana Res.* 59, 159–179.
- Safonova, I.Yu., Savinsky, I.A., Perfilova, A.A., Gurova, A.V., Maruyama, S., Tsujimori, T., 2020. Itmurundy accretionary complex (Northern Balkhash): geological structure, stratigraphy and tectonic origin. *Gondwana Res.* 79, 49–69.
- Safonova, I., Perfilova, A., Obut, O., Kotler, P., Aoki, S., Komiya, T., Wang, B., Sun, M., 2021. Traces of intra-oceanic arcs recorded in sandstones of eastern Kazakhstan: implications from U-Pb detrital zircon ages, geochemistry, and Nd-Hf isotopes. *Int. J. Earth Sci.* 111, 2449–2468.
- Safonova, I., Perfilova, A., Savinsky, I., Kotler, P., Sun, M., Wang, B., 2022. Sandstones of the Itmurundy accretionary complex, Central Kazakhstan, as archives of arc magmatism and subduction erosion: evidence from U-Pb zircon ages, geochemistry and Hf-Nd isotopes. *Gondwana Res.* 111, 35–52.
- Scholl, D.W., von Huene, R., 2007. Crustal recycling at modern subduction zones applied to the past - issues of growth and preservation of continental basement crust, mantle geochemistry, and supercontinent reconstruction. *Geol. Soc. Am. Mem.* 200, 9–32.
- Sengör, A.M.C., Natal'in, B.A., Burtman, V.S., 1993. Evolution of the Altaid tectonic collage and Paleozoic crustal growth in Eurasia. *Nature* 364, 299–307.
- Sennikov, N.V., Iwata, K., Ermikov, V.D., Obut, O.T., Khlebnikova, T.V., 2003. Oceanic sedimentation settings and fauna associations in the Paleozoic on the southern framing of the West Siberian Plate. *Russ. Geol. Geophys.* 44, 156–171.
- Sennikov, N.V., Obut, O.T., Bukolova, E.V., Tolmacheva, T.Yu., 2011. The depth of the early Paleozoic sedimentary basins of the Paleasian Ocean: lithofacies and bioindicator estimates. *Russ. Geol. Geophys.* 52, 1488–1516.
- Sennikov, N.V., Tolmacheva, T.Yu., Obut, O.T., Izokh, N.G., Lykova, E.V., 2015. Zonation of the Siberian Ordovician deposits based on pelagic groups of fauna. *Russ. Geol. Geophys.* 56, 761–781.
- Sennikov, N.V., Obut, O.T., Izokh, N.G., Kir'yanova, A.P., Lykova, E.V., Tolmacheva, T. Y., Khabibullina, R.A., 2018. The regional stratigraphic scheme of Ordovician deposits of the western part of the Altai-Sayan folded region (new version). *Geol. Min. Resour. Siberia* 7, 15–53.
- Shen, P., Pan, H., Seitmuratova, E., Yuan, F., Jakupova, S., 2015. A Cambrian intra-oceanic subduction system in the Bozshakol area, Kazakhstan. *Lithos* 224–225, 61–77.
- Shutov, V.D., 1967. Classification of sandstones. *Lithol. Miner. Resour.* 5, 86–102.
- Stern, R., 2010. The anatomy and ontogeny of modern intra-oceanic arc systems. In: Kusky, T.M., Zhai, M.G., Xiao, W. (Eds.), *The Evolving Continents: Understanding Processes of Continental Growth*, 338. Geol. Soc. London, Spec. Publ., pp. 7–34.
- Stern, R.J., Scholl, D.W., 2010. Yin and Yang of continental crust creation and destruction by plate tectonics. *Int. Geol. Rev.* 52, 1–31.
- Stratigraphic Code of Russia, Third edition, 2006. VSEGEI Press, Spb. 96 p. (Interdepartmental Stratigraphic Committee).
- Straub, S.M., Woodhead, J.D., Arculus, R.J., 2015. Temporal evolution of the Mariana arc: mantle wedge and subducted slab controls revealed with a tephra perspective. *J. Petrol.* 56, 1–31.
- Sun, S., McDonough, W.F., 1989. Chemical and isotopic systematics of oceanic basalts: implications for mantle composition and processes. In: Saunders, A.D., Norry, M.J. (Eds.), *Magmatism in the Ocean Basins*, 42. Geol. Soc. London, Spec. Pub., pp. 313–345.
- Sun, M., Yuan, C., Xiao, W., Long, X., Xia, X., Zhao, G., Kröner, A., 2008. Zircon U–Pb and Hf isotopic study of gneissic rocks from the Chinese Altai: Progressive accretionary history in the early to middle Palaeozoic. *Chem. Geol.* 247, 352–383.
- Tatsumi, Y., 2005. The subduction factory: how it operates in the evolving Earth. *Geol. Soc. Am. Today* 15, 4–10.
- Taylor, S.T., McLennan, S.M., 1985. *The Continental Crust: Composition and Evolution*. Blackwell, Oxford, p. 312.
- Ueda, H., 2005. Accretion and exhumation structures formed by deeply subducted seamounts in the Kamuikotan high-pressure-temperature zone, Hokkaido, Japan. *Tectonics* 24. <https://doi.org/10.1029/2004TC001690>. TC2007.
- Vladimirov, A.G., Kruk, N.N., Khromykh, S.V., Polyansky, O.P., Chervov, V.V., Vladimirov, V.G., Travin, A.V., Babin, G.A., Kuibida, M.L., Khomyakov, V.D., 2008. Permian magmatism and lithospheric deformation in the Altai caused by crustal and mantle thermal processes. *Russ. Geol. Geophys.* 49, 468–479.
- Wakita, K., 2012. Mappable features of mélanges derived from Ocean Plate Stratigraphy, in the Jurassic accretionary complexes of Mino and Chichibu terranes, Southwest Japan. *Tectonophysics* 568–569, 74–85.
- Wang, T., Xiao, W., Collins, W., Tong, Y., Hou, Z., He, H., Wang, X., Lin, S., Seltmann, R., Wang, C., Han, B., 2023. Quantitative characterization of orogens through isotopic mapping. *Nat. Commun. Earth Environ.* <https://doi.org/10.1038/s43247-023-00779-5>.
- Windley, B.F., Kröner, A., Guo, J., Qu, G., Li, Y., Zhang, C., 2002. Neoproterozoic to Palaeozoic geology of the Altai orogen, NW China: new zircon age data and tectonic evolution. *J. Geol.* 110, 719–739.
- Windley, B.F., Alexeev, D., Xiao, W., Kröner, A., Badarch, G., 2007. Tectonic models for accretion of the Central Asian Orogenic Belt. *J. Geol. Soc. Lond.* 164, 31–47.
- Xiao, W., Windley, B.F., Badarch, G., Sun, S., Li, J., Qin, K., Wang, Z., 2004. Palaeozoic accretionary and convergent tectonics of the southern Altai: implications for the growth of Central Asia. *J. Geol. Soc. Lond.* 161, 339–342.
- Xiao, W.J., Windley, B.F., Yuan, C., Sun, M., Han, C.M., Lin, S.F., Chen, H.L., Yan, Q.R., Liu, D.Y., Qin, K.Z., Li, J.L., Sun, S., 2009. Paleozoic multiple subduction-accretion processes of the southern Altai. *Am. J. Sci.* 309, 221–270.
- Xiao, W.J., Huang, B.C., Han, C.M., Sun, S., Li, J.L., 2010. A review of the western part of the Altai: a key to understanding the architecture of accretionary orogens. *Gondwana Res.* 18, 253–273.
- Xu, Z., Han, B.-F., Ren, R., Zhou, Y.-Z., Su, L., 2013. Palaeozoic multiphase magmatism at Barleik Mountain, southern West Junggar, Northwest China: implications for tectonic evolution of the West Junggar. *Int. Geol. Rev.* 55, 633–656.
- Yang, T.N., Li, J.Y., Zhang, J., Hou, K.J., 2011. The Altai-Mongolia terrane in the Central Asian Orogenic Belt (CAOB): A peri-Gondwana one? Evidence from zircon U–Pb, Hf isotopes and REE abundance. *Precambrian Res.* 187, 79–98.
- Yang, Y.Q., Zhao, L., Zheng, R.G., Xu, Q.Q., 2019. Evolution of the Early Paleozoic Hongguleleng–Balkybay Ocean: Evidence from the Hebukesaier ophiolitic mélange in the northern West Junggar, NW China. *Lithos* 324–325, 519–536.
- Zhang, J., Xiao, W., Luo, J., Chen, Y., Windley, B.F., Song, D., Han, C., Safonova, I., 2018. Collision of the Tacheng block with the Mayile-Barleik-Tangbale accretionary complex in Western Junggar, NW China: Implication for Early-Middle Paleozoic architecture of the western Altai. *J. Asian Earth Sci.* 159, 259–278.
- Zheng, R.G., Zhao, L., Yang, Y.Q., 2019. Geochronology, geochemistry and tectonic implications of a new ophiolitic mélange in the northern West Junggar, NW China. *Gondwana Res.* 74, 237–250.
- Zonenshain, L.P., Kuzmin, M.I., Natapov, L.M., 1990. Geology of the USSR: A Plate Tectonic Synthesis. In: *Geodynamic Monograph Series*. Am. Geoph. Union, 328 p.